Experimental Virtual Reality Framework to Study Individual Pedestrians Avoidance of Pedestrian Groups in Crowded Situations.

Joel Patane – Bachelor of Information Technology

6th June 2016

Dissertation submitted by Joel Patane in partial fulfilment of the requirements for the Degree of Bachelor of Information Technology with Honours in the Department of Information Technology, School of Business at James Cook University.

Declaration

I, Joel Patane, declare that this thesis is my own work and has not been submitted in any form for another degree or diploma at any university or other institute of tertiary education. Information derived from the published and unpublished work of others has been acknowledged in the text and a list of references is given.

Date: 6th June 2016

Abstract

A completely wireless virtual reality framework that allows users to control virtual avatars by physically walking is becoming increasingly necessary as virtual reality technologies such as the Oculus Rift and HTC Vive are pushed into the mainstream market. Virtual reality is no longer an expensive tool only employed by the better funded researchers. To this end we proposed to create a novel virtual reality framework which lays the ground work for future researchers to utilize. The use of our virtual reality framework for research is validated through a virtual reality study which aims to help fill the knowledge gap of how individual pedestrians navigate through crowds. As a result of conducting our virtual reality experiment we have confirmed that our virtual reality framework is capable of observing qualitatively similar collision avoidance decisions of individual pedestrians when compared to previous researcher's results. Additionally, we have confirmed the presence of a distance compression effect in virtual reality; increased gait instability, and modified personal space of users inside virtual worlds. Our virtual reality framework was positively received with an enjoyment score of 5.6 out of 7(7 being very enjoyable).

Acknowledgements

I would like to thank my supervisor, Doctor Carrie Lui for her guidance and helpfulness throughout my Honours year. Her encouragement and incite during tough times was what gave me the boost that I needed to complete the year. I would also like to thank Doctor Jason Holdsworth for taking on the role of supervisor for two of my special topic subject at such short notice. Additionally, I would like to thank both Jason and Doctor Joanne Lee for being very supportive and allowing the submission of the thesis to be flexible.

Contents

Figures

1 Introduction

Crowd simulation is the process of simulating the movements of large numbers of virtual agents. Crowd simulations are used for a wide variety of applications, from being used for entertainment purposes; in movies and videogames, to assisting in architecture during building analysis and emergency evacuation studies. With such important application fields the scientific community has put a lot of effort into developing more and more realistic crowd simulation algorithms.

In the past researchers have used their intuition for determining the behavioural rules for agents in crowd simulations. However, this often leads to unrealistic and un-validated crowd simulation models. Real world data needs to be collected in order to develop realistic virtual agents, scenarios and environments for crowd simulations. Virtual reality is a powerful and convenient tool which can be utilised to obtain qualitatively realistic pedestrian trajectories, navigation decision and collision avoidance decisions; which can be used to improve upon future crowd simulation algorithms.

A completely wireless virtual reality framework that allows users to control virtual avatars by physically walking is becoming increasingly necessary as virtual reality technologies such as the Oculus Rift and HTC Vive are pushed into the mainstream market. Virtual reality is no longer an expensive tool only employed by the better funded researchers. To this end we proposed to create a novel virtual reality framework which lays the ground work for future researchers to utilize. The use of our virtual reality framework for research is validated through a virtual reality study which aims to help fill the knowledge gap of how individual pedestrians navigate through crowds.

From our research, we found that we were able to further prove the distance compression effect in virtual reality [15, 16, 17], increased gait instability [27] and modified personal space of participants [26, 19]. Our Virtual reality framework was positively received with an enjoyment score of 5.6 out of 7(7 being very enjoyable).

1.1 Significance of Research and Problem Statement

Many studies have investigated how pedestrians navigate as a group- this makes sense as according to the research the majority of people in a crowd are comprised of groups of people [7]. There is a very obvious research gap with only one very recent paper produced by Bruneau specifically investigating how individual pedestrians avoid crowds [12]. We propose to improve upon the previous work in this area through the use of our virtual reality framework and realistic virtual agent groups based on the findings of Moussaid [7]. Virtual reality has been proven to be a powerful tool for qualitative research [1] [12], and with it recently becoming more accessible and affordable, a solid framework needs to designed for future virtual reality studies. We propose to create such a framework, which will enable avatar control through actually physically walking.

1.2 Aims

In this paper we seek to create a completely wireless full body virtual reality framework which will be validated through a virtual reality study investigating how individual pedestrians navigate through virtual crowds. This framework will lay the ground work for future research that can benefit from using a full body virtual reality system, such as additional investigation of individual pedestrians behaviours and decisions. We aim to implement an automated data collection system which will enable us to recreate the movements of the virtual crowd and the participant in a visualisation. The visualisation will allow us to visually observe with perfect precision the collision avoidance decisions and behaviours of each participant.

Our contributions include:

1. Production of a completely wireless full body virtual reality framework which can be utilized for future research.
2. Investigation of how individual pedestrians navigate through crowds of realistic group formations with different visual appearances.

1.3 Thesis Structure

The thesis structure is as follows:

- Chapter 2 details preliminary information pertaining to crowd simulation. Chapter 2 also explores the current literature of using virtual reality systems for human locomotion behaviour research; exploring pedestrian group dynamics and the limitations of virtual reality and other more conventional pedestrian data gathering methods.
- Chapter 3 explored both the hardware and software implementation of our virtual reality framework.
- Chapter 4 phase1 investigates the amount of spatial drift of our inertial motion sensor based motion capture suit.
- Chapter 4 phase 2 puts our virtual reality framework to the test by using it to investigate how individual pedestrians navigate crowds.
- Chapter 5 discusses the results from our virtual reality study and validates our virtual reality framework.
- Chapter 6 summarises our research and explored future directions of our work.

2 Preliminaries

2.1 Crowd Simulation

Crowd simulation is the process of simulating the movements of large numbers of virtual agents. Crowd simulation modelling has been extensively researched by the scientific community for decades. Crowd simulations have a wide variety of applications like being used for entertainment purposes in movies and videogames, assisting in architecture; during building analysis, and emergency evacuation studies. With such important application fields the scientific community has put a lot of effort into developing more and more realistic crowd simulation algorithms.

2.2 Macroscopic and Microscopic models

In the last few decades there has been a greater focus on developing more accurate and realistic microscopic models for crowd simulations. Microscopic pedestrian simulation models are based on local interactions between agents. Conversely, macroscopic pedestrian simulations are often described as behaving like a liquid or a gas. Macroscopic models consider pedestrians as a whole, ignoring the local dynamics of individuals and their interactions between other pedestrians or obstacles. Therefore, macroscopic models have a massive computational load advantage over microscopic approaches which need to perform individual calculations for each pedestrian agent [3].

Researchers found that the macroscopic models were not capturing enough of the psychological behaviour of real pedestrians. Fluid molecules, for example, do not have a need for personal space between themselves, nor are they distracted by interesting events while moving, whereas, people prefer to maintain some personal distance between themselves and they also have the capacity to be distracted by various events; such as pausing to take a photo of an expensive and rare motor vehicle[2]. Additionally, macroscopic models often assume that the population is made up of homogenous agents, which is not accurate for real-world situations [4].

Microscopic models focus on the individual behaviours and decision making of each pedestrian agent. This attention to the finer details of pedestrian dynamics allows microscopic models to overcome the limitations of macroscopic models. If the microscopic model properly defines a set of predetermined behavioural rules they will create more realistic pedestrian behaviour in a larger variety of situations than macroscopic models [5], [6]. However, in-order to obtain these rules, rich data sets need to be analysed. In the last 20 years, advances in technology have allowed for such datasets to be produced [4].

2.3 Common microscopic models

2.3.1 Social Force Models

The social force model for crowd simulation was initially proposed by Helbing where he defined the basic equation of the social force model to simulate pedestrian motion. Helbing’s model gives virtual agents four different motivational factors that influence a pedestrian's motion. These are as follows:

1. The desire of the pedestrian to reach a certain destination or goal,
2. The influence from other pedestrians, such as their repulsive effect,
3. The total repulsive force created to avoid a boundary or an obstacle,
4. The attraction level of other pedestrians or objects [20].

2.3.2 Cellular Automata Models

Cellular automata is a novel model for crowd simulation. [3] In cellular automata models, the simulation world is defined by a uniform grid of cells. At each discrete time step, the values of variables in each cell are updated according to a set of local rules and the values of the variables in the cells in its neighbourhood [21].

2.3.3 Agent-Based Models

Agent-based crowd simulation is made up of autonomous decision-making agents [3]. The agents in agent-based models follow predetermined behavioural rules that allow the agents to perform various behaviours appropriately in crowd simulations. This characteristic makes agent-based models particularly useful for the study of pedestrian behaviours in complex environments [3].

2.3.4 Reciprocal Velocity Objects.

This model is able to simultaneously determine actions for thousands of agents, which each may have different objectives. These actions are computed independently for each agent, there is no agent to agent communication or central communication. Yet the model maintains collision free motion for each of the agents. Agents avoid collisions with each other by independently and simultaneously selecting a new velocity for itself, so that all of the agents are guaranteed to be collision free. However, each agent is making the assumption that the other agents are using the same strategy as they are when they select a new velocity. [24]

2 Literature Review

2.1 Data Collection for Crowd Simulations

In the past researchers have used their intuition for determining the behavioural rules for agents in crowd simulations. However, this often leads to unrealistic and un-validated crowd simulation models. Real world data needs to be collected in order to develop realistic virtual agents, scenarios and environments for crowd simulations. Realistic crowd simulations are used for entertainment purposes; in movies and videogames, assisting in architecture; during building analysis and emergency evacuation studies. With such important application fields it is important to ensure that the data for these simulations is validated by coming from real world video analysis[7,8,9,10,11] or through people participating in realistic virtual reality simulations[12,1, 19].

2.1.1 Video Recording Analysis:

Video recording analysis provide researchers with a visual copy of the real world, which provides physical and visual data. Moussaid used video recording analysis of 1500 pedestrians to obtain empirical data on pedestrian groups walking formations [7]. Moussaids findings were used to simulate the local behaviour of small pedestrian groups, which were then validated quantitatively through several metrics which were benchmarked against real world data [22].

Video recording analysis provides researchers with the following benefits:

- Is easier to validate findings as it is 100% real life.
- Can easily study group and individual pedestrians.
- Is very good at investigating simple behaviours/ variables in crowded situations, such as pedestrian speed, group dynamics, impacts of density, etc.

Although video recording analysis can obtain good data it does have some drawbacks:

- It can suffer from a lack of precision [1].
- Researchers are often left wondering about people state's/motivations [1].

- Includes uncontrolled elements [1].
- Almost impossible to study specific pedestrian behaviours, such as the impacts of other pedestrian appearance/speed/behaviour, different motivations etc. on pedestrians navigation behaviours.
- Data collection is not automatic
  - *Note video analysis is beginning to become more automatic* [23]. *However, automatic data collected using video analysis pales in comparison to what can be collected automatically using virtual reality.*

2.1.2 Virtual Reality:

Virtual reality simulations require real people to move inside a virtual world where the researcher can gather data on the person's movements, actions, and decisions.

Virtual reality is prevalent in two forms; cave automated virtual environment (CAVE) and head mounted display (HMD). Previous research has shown virtual reality to be a powerful and convenient tool for investigating pedestrian behaviours and collision avoidance strategies. Previous work has proven virtual reality to be capable of obtaining qualitatively realistic data, such as collision avoidance strategies and navigation decisions.

Bruneau collected qualitative decision making data (go through crowd or around crowd) about how individual pedestrians navigate through a virtual crowd using a joystick and 4 wall CAVE. Bruneau used the collected data to modify the RVO2 crowd simulation framework with some new behavioural algorithms which embodied their participant's navigation decisions. Bruneau validated the new algorithms through a user study, finding that the new algorithms where perceived to be performing more realistic collision avoidance than the base RVO2 model [12].

Olivier conducted a comprehensive virtual reality study that mimicked the real world works of [13, 14]'s study which investigated the collision avoidance between two real pedestrian walkers. Olivier found that virtual reality simulations are able to provide qualitatively realistic avoidance trajectories. Olivier observed quantitative differences in avoidance distances, where the participants slightly over-adapted their trajectories, possibly due to the different distance perception in VR [16].

Bruneau and Olivier's works ultimately prove that virtual reality can provide reliable results for qualitative analysis, such as collision avoidance strategies and navigation decisions [1][12].

Virtual reality allows researchers to investigate pedestrian behaviour with great efficiency and effectiveness because of the following:

- Only need one participant to observe individual behaviour in crowded situations.
- Can accurately control and repeat a virtual reality experience over several participants.
- Can accurately measure each individual participant's data.
- Can easily and quickly manipulate factors in the simulation experience to observe their effects on the participants behaviour.
- Automatic data collection.

However, virtual reality is not without its weaknesses:

- The world is perceived through a digital display which negatively influences participant's visual perception, described as a distance compression effect [15, 16, and 17].
- Distorted movement velocity when compared to real life [18].
- Using gamepads/ joysticks for movement is too different to the actual walking motion, adding some bias to any results.[1]

Motion tracking equipment can be utilized to allow users to control their virtual avatars by physically walking. This can remove the bias introduced by the use of gamepads or joysticks. Although, more realistic for the participant researchers have shown that controlling avatars by physically walking does not lead to quantitative data collection; the walking speed is reduced [25], personal space size is modified [26],[19] and navigation in virtual reality is performed with increase gait instability [27].

2.2 Collision Avoidance; Individual vs Group:

There have been many studies investigating and simulating how people navigate together as a group [7, 8, 10, 11]. This makes sense, as according to Moussaids research, the majority of pedestrian crowds are made up of small groups, up to 70% in fact[7]. However, we still need to know how the minority interacts with the majority. Bruneau is one of the few researchers who have looked into specifically answering this question. Bruneau conducted a virtual reality study where he found that his 13 participants followed the rules of The Principle of Minimum energy (PME). PME states that humans tend to optimize their trajectory to use as little energy as possible to reach their goals [12]. Nonetheless, there was still some inconclusive situations which could not be defined by the PME, where both solution paths have the same or similar energetic cost. To evaluate these inconclusive situations Julian introduced two factors to help influence a decision from the participants; group appearance and group direction of motion.

Pedestrian group formations discussed in the next heading, could play an important role in an individual's avoidance of groups, we do not know for sure because it has not been fully investigated yet. Additionally, the appearance of crowds has been shown to have some effect on an individual participant's avoidance strategies [12].

2.3 Crowd Formations/ Shapes

Moussaid analysed empirical data in the form of video recordings of the motion of pedestrian groups in public areas. The results of the analysis of the data, found new information regarding pedestrian group dynamics. Discovering that up to 70% of pedestrians are moving in small groups, made up of 2-4 friends, family or acquaintances [7]. Interestingly, Moussaid also observed the pedestrians in these groups moving in formations which are dependent on the density of the crowds. The following three distinct walking formations were observed (Figure 2-1):

1. Pedestrians tend to walk in the “Line abreast” formation whenever the density of the upcoming obstacles allows. This formation allows pedestrian groups to easily communicate with each other as they advance towards their goal [7]. Additionally, the “Line abreast” formation has been observed

in the works of Perters who analysed video recordings of the motion of pedestrian groups in order to develop natural crowd simulations [8]. Koster conducted a study in which 30 students were told to leave a room through the exit at the same time; once through the door (bottleneck), the students formed “line abreast” formations [11].

2. When the crowd and/or obstacle density is moderate, the pedestrian group’s space is reduced, forcing a change in walking formation to the “V-like” formation, facilitating the social communication between the group members. For groups of two pedestrians, the “V-like” formation is replaced by a more compact “Line abreast” formation, in which the distance between the two group members is significantly reduced [7]. References to the “V-like” pedestrian formation was also observed in Perters work [8].
3. During high crowd and/or obstacle density, the need for safety overcomes the want of social communication and interaction. This results in the “River like” formation (leader follower model) [7], which is corroborated by Kretz who was using participants to test the effects of pedestrian flow and counter-flow in a corridor. They observed “lane formation” where the participants chose to follow the person in front of them when the density of the crowd has high [9]. Singh observed the river-like formations while investigating video footage, with the purpose of understanding pedestrian group and subgroup behaviour [10]. Koster observed the river-like formation being formed when pedestrians are moving through a doorway (bottleneck).

Figure 2-1: Moussaid’s three group formations [7].

When developing a simulation experiment that includes virtual crowds it is important to ensure that all of the key elements are perceived by the participants as being as similar to what they encounter in real life. For this reason, Moussaid's research into group formations will play a key part in the design of our groups of virtual agents, which will reflect [7]'s three group formations; "line abreast", "v-like' and "river-like".

2.4 Crowd density

In crowd simulations, density refers to the closeness that the virtual pedestrians are to each other in crowds or groups. The density of crowds and groups can have significant effects on the behaviour of individual pedestrian's navigation decisions.

Studies evaluating the use of virtual reality to study human personal space behaviour, has shown that participants maintain personal space bubbles around virtual humans which are qualitatively the same as the bubbles typically maintained around actual humans [19]. Research has found that the speed of real pedestrians is clearly dependant on the density level of the crowd. At low density pedestrians were observed moving faster than at a high density [7]. It has been found, that, on average, low density crowds are traversed by the majority of individuals and, high density crowds are avoided as a whole [12].

Through the use of Moussaids three group formations we will be inherently studying the effects of density on an individual's avoidance of crowds. Although, we do not expect to see any significant differences in results between our findings and Moussaids and Bruneaus[7, 12]. However, it will be interesting to study the impacts of using realistic group formations on an individual's avoidance behaviour.

2.5 Crowd appearance

The appearance of an approaching crowd can have an impact on an individual’s or even a group’s avoidance decisions and behaviour. Understanding the impacts of appearance on an individual's avoidance decisions and behaviour is an important area of study for microscopic crowd simulations. Where each agent will have different decisions and behaviour to its neighbours. Researching how changes in appearance affect an individual participant will help define the rules for future microscopic crowd simulation models. When avoiding a collision the virtual agents can take into consideration the rules when “thinking” about a navigational or behaviour decision (go through, go around, slow down etc...).

Research into the personal space people give to individual virtual agents has revealed that people give more personal space to the individual agents who engaged them in a mutual gaze [19] verses those that had their eyes closed. This research can be expanded upon by investigating how an individual would react to a group of virtual agents facing the individual as they walk towards them. Will the virtual agents facing them have a significant impact on the avoidance behaviour of participants? Additionally, instead of having the virtual people close their eyes, we perform a more realistic alternative by investigating how an individual will navigate groups of virtual agents with their back facing the participants.

Bruneau investigated the impact of crowds having an easily distinguishable social-link with each other. They did this using a crowd of soldiers, finding that more of their participants went around the group of soldiers than going through [12]. However, Bruneau’s simulation lacked the pedestrian group formations observed by Moussaid [7]. It would be interesting to investigate if there is a qualitative difference in avoidance decision when faced with realistic group formations.

There is some discrepancies in the literature related to using virtual reality to study the impacts of a virtual person's appearance on participants. Bruneau also studied the impact of repulsion on his participants by using zombie models. Bruneau and I (when I read the paper) expected to see the majority of the participants completely circumventing the zombie virtual agents. However, this was not the case; in-fact, just less than half of his participants completely avoided the zombie appearing agents. He hypothesised that the reason for this was that his participants knew the zombies were not real. This is a dangerous hypothesis and it can negatively impact studying the effects of virtual people's appearance on participants using virtual reality. Additionally, Bruneau's differences in results for each appearance, normal, zombie and social-link were separated from each other by a difference of less than 10%; which is disappointing and I believe could be linked to his participants knowing that the virtual agents were not real. We hope to observe greater differences when we study the impacts of appearance by creating a more realistic virtual reality simulation, enabling participants to control their virtual avatars by physically walking in the real world.

3 Implementation

In chapter 2 we focused on investigating the literature of using virtual reality systems for human behaviour research; exploring pedestrian group dynamics and limitations of using both virtual reality and more conventional pedestrian data gathering methods for investigating pedestrian behaviours. Using the literature from the previous chapter we investigate the implementation of a new novel experimental virtual reality framework to be used to investigate how an individual navigates through crowds.

3.1 Hardware Implementation

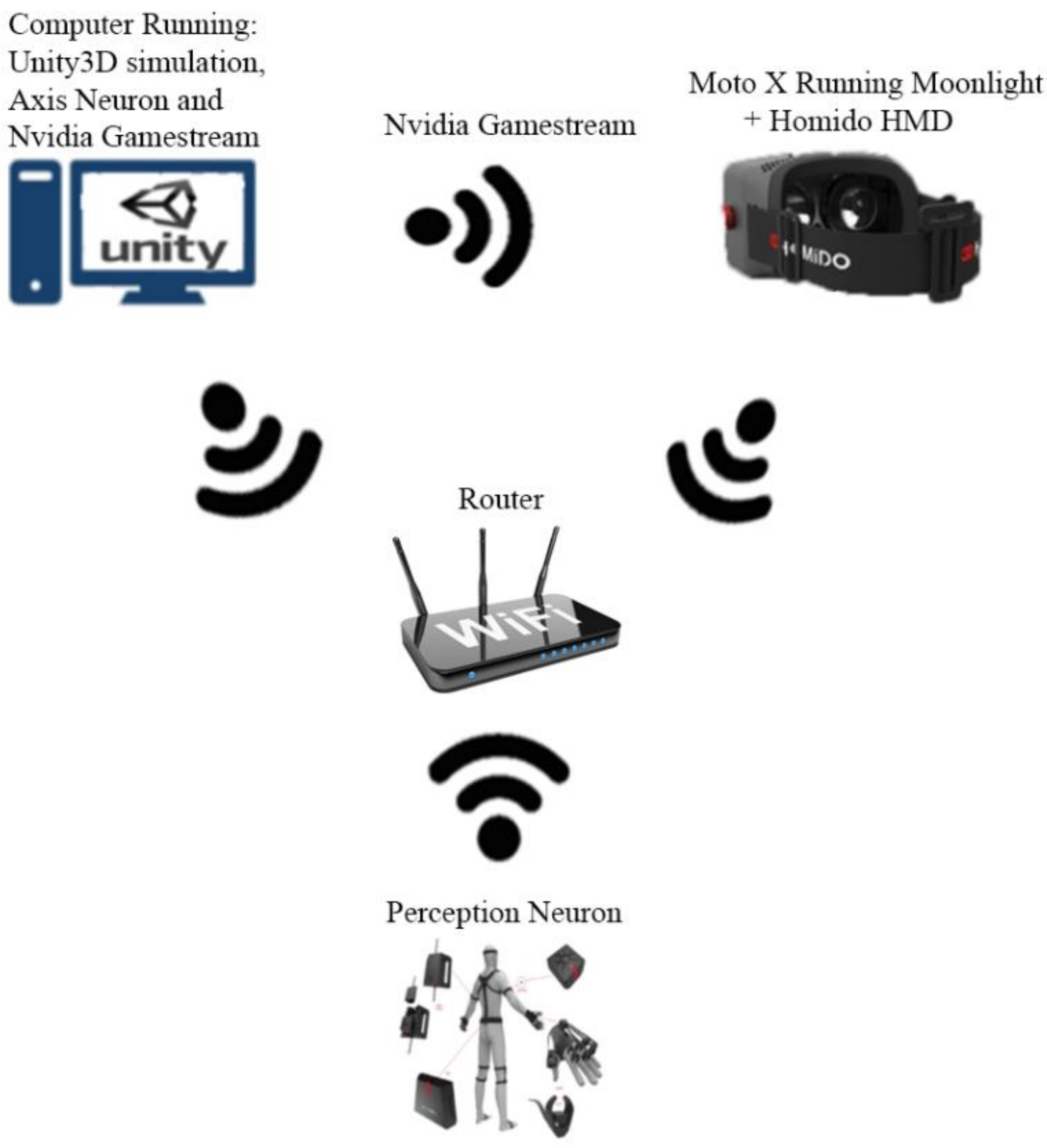

Figure 3-1: Hardware implementation.

The hardware components of the system Include the Perception Neuron full body 18 Neuron motion capture kit, head mounted display (Moto X 2nd Gen mobile) and High performance desktop computer. These components are all connected to each other wirelessly to allow the participants un-restricted movement.

- The computer is running the Axis Neuron software which interprets the data sent by the Perception Neuron kit to create the motion capture.
- The computer is using Nvidia GameStream technology to stream the Unity3D virtual reality simulation to the mobile display (Moto X 2nd Gen) running Moonlight (open source implementation of Nvidia GameStream for Android devices).
- The screen from the mobile (Moto X 2nd Gen) is being used as the display for the Homido head mounted display.

Figure 3-2: The Perception Neuron motion capture kit and head mounted display being used during the experiment.

3.1.1 Perception Neuron; Motion capture sensor suit

Perception Neuron is an inertial motion sensor based motion capture system. The system uses inertial motion unit data fusion, human body dynamics and physical engine algorithms to deliver smooth and accurate motion capture. The inertial motion unit based sensors in the suit are called “Neurons” which are attached to the limbs of the body using velcro straps and are also connected to the Hub device via cables. Due to inertial motion unit’s tendency to experience spatial drift overtime, each Neuron performs some drift correction before the data from each of the Neurons are gathered by the hub device and transmitted via WI-FI (or USB) to a computer running the Axis Neuron software. The Axis Neuron software then performs some data optimization and more drift correction before reconstructing a human skeleton comprised of 59 bones from the inertial motion unit data from the Neurons. This data is then sent as binary float values to the Unity3D game engine to drive the motion of the participant’s virtual avatar [31].

3.1.2 Inertial Motion Unit Drift Correction

The inertial motion units inside each of the Neurons include a 3 axis accelerometer, 3 axis magnetometer and a 3 axis gyroscope. The data from each of these sensors is being used together, in a process called data fusion to determine the orientation, velocity and displacement of the inertial motion units in a global frame of reference [29].

Accelerometers and gyroscopes are used in inertial motion units as a baseline to determine the orientation with respect to a given body frame of reference. Gyroscopes sense orientation through angular velocity changes and subsequently find the orientation. However, gyroscopes have a tendency to drift over time due to only sensing the changes and having no fixed point of reference. The addition of an accelerometer reduces the drift of the gyroscope to be minimal. The accelerometer achieves this by giving the gyroscope a sense of gravity- which orients the gyroscope to a more exact angular displacement. Accelerometers are better at determining orientation when the device is closer to its fixed reference point, whereas gyroscopes are better at determining orientation when the device is in motion. Accelerometer sensors tend to distort accelerations due to gravity influencing the external force moving the mass when the accelerometer is in motion. The distortion accumulates as noise and erroneous spikes in the output. Together; a gyroscopes longer-term accuracy combined with the shorter term accuracy of an accelerometer provide more accurate orientation readings by utilizing the benefits from each sensor [30]. A magnetometer can be used to further reduce the drift of the device. Magnetometers find the direction of magnetic north. Magnetometers are not as accurate as gyroscopes. However, their data can be added to the gyroscopes data to improve the accuracy of the calculated orientation- by telling the gyroscope which way is north [29].

Data fusion and possibly other drift correction strategies or algorithms that are not advertised by the Perception Neuron developers is not enough to prevent an inertial motion sensor from experiencing drift overtime. Perception Neuron's inertial motion sensors are no different. However, the spatial drift overtime is minimal (see chapter 4.1 for analysis of the drift).

3.1.3 Latency

The Perception Neuron system is comprised of many components each adding to the overall input latency of the system. It is important for any 3D games or simulations, virtual or otherwise for there to be low input latency.

- The calculation of the on-board Neuron microcontroller unit has a measured latency of 10-13ms.
- The data transmission from the Hub to Computer has a reported latency of ~8ms(USB) and ~25ms(Wi-FI) [32].
- The calculation in the Axis Neuron Software has an average latency of 3-5ms(depends on processing power of CPU, in our case we used a FX 8350)

Overall the Perception Neuron kit has an input latency of roughly 26ms if the Hub is connected to the computer via USB, and 43ms of latency over a WI-FI connection. For comparison a basic (non-gaming edition mouse) in Windows 7 has a measured input latency of 8ms and a gaming-edition mouse has an input latency of 1ms. There is still a ways to go for the Perception Neuron to reach a similar input latency that we are currently seeing in standard mouses. However, it should be noted that this kind of virtual reality technology is very new (Idea Proposed in 2014 via a kick-starter campaign and in the future it will become both more accurate in terms of drift correction and faster for reduced latency.

3.1.4 Homido; Head Mounted Display (HMD)

The Homido is a completely wireless HMD allowing the users to have total freedom of movement. The Homido is a low cost head mounted display, the display of the Homido is powered by a high powered mobile phone (Motorola Moto x 2nd gen) with a 1080p screen with a 60Hz refresh rate which means the latency between each displayed frame is 16.67ms. This particular combo has similar specs to the Oculus rift DK2 which both have a display providing a resolution of 960X1080 for each eye. Both the Oculus Dk2 and the Homido feature custom virtual reality lenses that provide the wearer with a 100 degrees field of view. The only important difference between the Oculus Dk2 and out Homido + Moto X combo is the Oculus

Dk2's higher refresh rate on their display, 75Hz which means the latency between each displayed frame is 13.33ms.

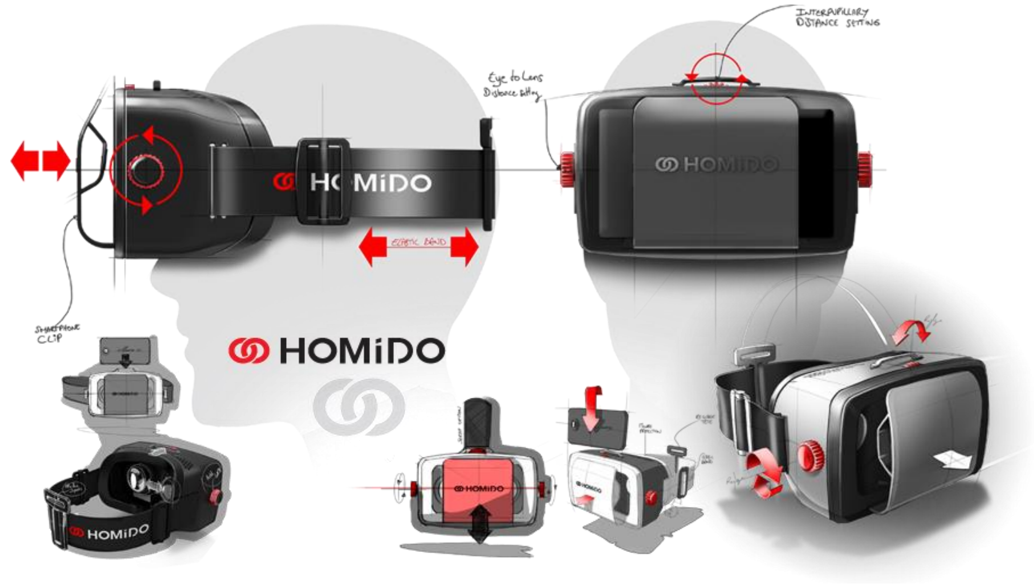

Figure 3-3: Homido Diagram

The Homido is the logical choice for the experiment due to its similar specs to the DK2 and its ability to be completely wireless. While it is possible to force the oculus rift to become wireless by using a wireless HDMI transmitter and receiver there would still be latency, albeit possibly a few milliseconds smaller, but it would not be worth the cost of implementing. Furthermore, since the specifications of our Homido + Moto X combo and the Oculus Dk2 are more or less the same the only benefit to using the Oculus Dk2 would be the fact that it is more comfortable on the head than the Homido.

3.1.5 Moonlight NVIDIA GameStream:

Moonlight is an open source implementation of NVIDIA's GameStream, used by the NVIDIA Shield devices. Moonlight reverse engineered the Shield streaming software and created a version that can be run on any Android device.

An NVidia GTX 970 was used on the computer to run the virtual reality simulation and stream the video feed to Moonlight running on the Motorola Moto X 2nd gen. The Moto X and the computer where both connected to a 300Mbs 2.4 GHz band router. The computer was connected to the router with an Ethernet cable providing a connection speed of 100Mbs and the phone was connected wirelessly providing a connection speed of 72Mbs.

Moonlight streamed the simulation to the Moto x at a resolution of 1280x720 with a frame rate per second (FPS) of 60 and a default target video bit-rate of 10Mbs. I found these settings to provide the best experience for the user. Bumping the resolution to 1920x1080 and a FPS of 60 with a default target video bit-rate of 20Mbs gave a slight and unpredictable stutter that was very noticeable during head tacking when user was rotating their head. Streaming at 720p with 60FPS has an average frame decoder latency of ~12ms, while streaming at 1080p with 60FPS gave an average frame decoding latency of ~24ms. The video was encoded using the H.264 standard instead of the more superior H.265 standard, H.265 is reported to give up to double the performance of the previous H.264 standard [33]. Unfortunately, even though both the GTX 970 and Moto X are supposed to support the H.265 standard Moonlight would fail to find the H.265 decoder on the Moto X when it was selected in the settings.

3.1.6 Evaluation of the overall latency

A variety of sources combine to result in an overall latency of roughly up to 89.67ms for our virtual reality system. The breakdown is as follows:

- The calculation of the on-board Neuron microcontroller unit has a measured latency of **10-13ms.**
- The Data transmission from Hub to Computer has a reported latency of ~**25ms (Wi-FI)** [32].
- Calculation in Axis Neuron Software has an average latency of **3-5ms**(depends on processing power of CPU, In our case we used an FX8350)
- Graphical rendering latency depends on end usage program, in our case Unity3D and has a measured latency of roughly **(15-18ms)** depends on how many agents are in view of the avatar.
- Latency of the display being used, in our case we are using a mobile display with a refresh rate of 60Hz, which means it will take 16.67ms for each frame to be displayed- it should be noted that the simulation was running at above 60 FPS on the host computer and is being streamed at 60FPS to the mobile device inside the Homido with an average frame decoder latency of **~12ms**.

Therefore, we have an estimated measured latency of up to 10+25+3 to5+15 to 18+16.67+12= 81.67ms to 89.67ms. This means that it takes roughly up to 0.089 seconds for the participant's movements to be reflected by the system. It should be noted that this is also the latency of the head tracking of the participants as we are using the rotation data from the head mounted Neuron to update the rotation of the stereoscopic camera in Unity3D. It is expected that the high latency for the head tracking will add some bias to the experiments conducted and will be discussed in chapter 4.2.3.2

3.2 Software Implementation

In this chapter we are discussing the implementation of all of the software components of our virtual reality framework. The software elements include the virtual agent's implementation, the implementation of stereoscopic 3D vision and head tracking, and the integration of the Perception Neuron kit into Unity3D.

3.2.1 Virtual Agents Technology

Realistic virtual agent navigation is important for the integrity of an experiment that is using virtual people to investigate a real persons navigation decisions. It was also the hardest component to implement. We chose to use a Reciprocal Velocity Obstacles (RVO) based pathfinding implementation for our virtual agent's navigation. The reason for this is that during a collision avoidance situation both agents work together to avoid a collision, this is similar to the behaviour observed in a study comparing the walking trajectories of 2 walkers on a collision course with each other [13].

3.2.1.1 A* Pathfinding Project for Unity 3D; Local Avoidance

The agents in the virtual reality simulation are being driven by the Local Avoidance system included within the A* Pathfinding Project for Unity 3D, which is based on RVO: Reciprocal Velocity Obstacles. The RVO Implementation is sampling based and uses gradient descent to find the optimal velocity for the agents [34].

The local avoidance system in the A* Pathfinding Project for Unity 3D is based on the works of Jur van den Berg who proposed the concept of Reciprocal Velocity Obstacles for real-time multi-agent navigation. When performing collision avoidance RVO agents implicitly assume that the other RVO agents will make similar collision avoidance decisions. Essentially, the agents both adjust their speed, and direction to avoid colliding with each other. RVO guarantees safe and oscillation free motion for the agents [35].

3.2.1.2 A* Pathfinding Local Avoidance Performance

The A* Pathfinding Project for Unity 3D is capable of simulating 5,000 agents at 20fps if the simulation is powered by a powerful enough central processing unit (CPU). It should be noted that the visualisation for this performance test was done by creating a mesh which held one quad for each agent. The reason for this is that at such a high number of agents, creating a GameObject for each agent is a slow process, just creating that many game objects took about 10 seconds. The agents were arranged in a circle and are tasked with moving towards their antipodal points [34] (Figure 3-4).

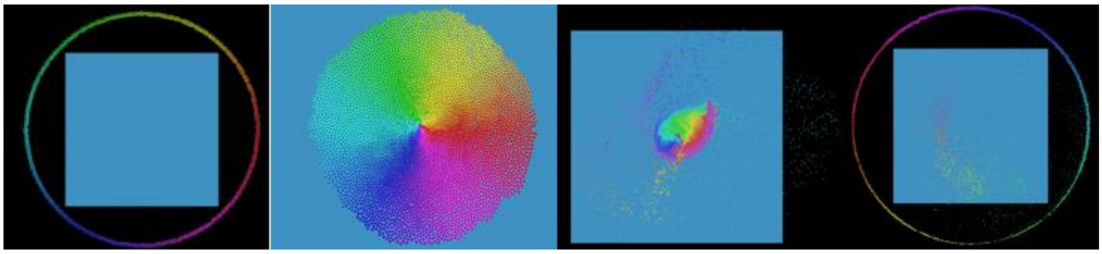

Figure 3-4: A Pathfinding Local Avoidance performance test.*

An AMD FX 8350 central processing unit was used to run the simulation with 5,000 agents at a comfortable 55-60 fps (frame rate capped at 60fps). However, With 10,000 agents the frame-rate dropped to 10-15 fps. The steep decline in frame-rate shows that this particular implementation of RVO is best suited to a maximum of 5,000 agents. However, the scalability of the A* Pathfinding projects RVO implementation does not limit my experiment as I only need about 50 agents to be active at once during the crowd simulation.

3.2.1.3 Limitations of A* Pathfinding Local Avoidance

A* Local Avoidance is not the golden gun for crowd simulation, it comes with a few glaring limitations:

1. The local avoidance system only considers obstacles a few seconds into the future. This leads to agents being forced through obstacles, or each other. For example, if two agents meet in a very thin corridor one of the agents will be pushed through the obstacle to make room for the other. The yellow circles indicate the radius of the RVO Collider, the red boxes are the obstacle points. As you can see the agents are forced through the obstacles. If the system had longer term planning it might be able to resolve the situation by not getting into the situation in the first place. However, having the agents push through the obstacles is still better than the agents being stuck in the corridor because there is no space(Figure 3-5).

   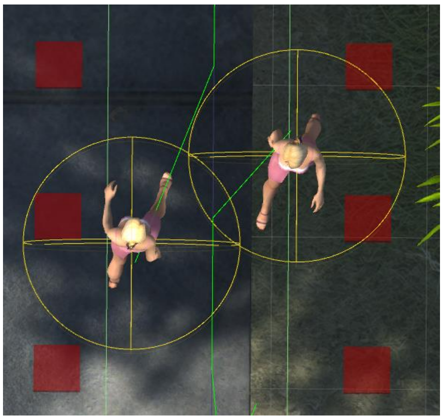

   Figure 3-5: A Pathfinding Local Avoidance has a tendency to push through wall and each other in dense environments.*

2. Powerful, but unrealistic avoidance in densely packed environments. For example; in a scenario where there are two lines of densely packed agents moving to opposite sides of the screen (Figure 3-6, Fig1). The avoidance behaviour of the system in this scenario, is not very realistic with the agents avoiding around the opposite line of agents one by one on the ends (Figure 3-6, Fig2). Realistically, the agents should be following the findings of Moussaids research into

the walking behaviour of pedestrian groups; splitting into river-like or at least v-like formations to allow more space for the agents to smoothly avoid each other(Figure 3-6, Fig3)[7].

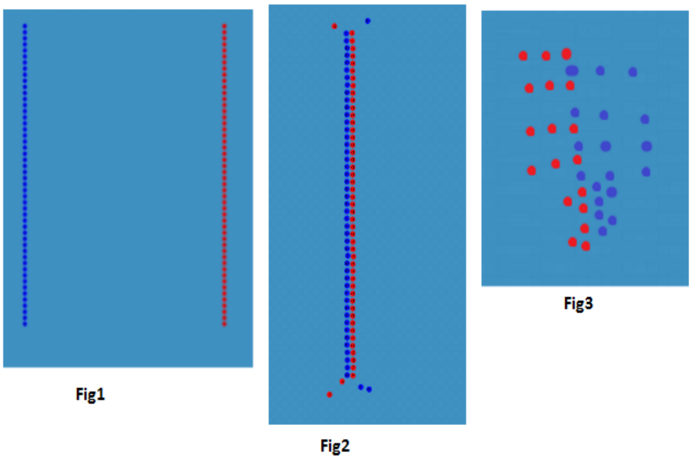

Figure 3-6: A Pathfinding Local Avoidance does not follow Moussaids observed formations.*

3.2.2 Virtual Agents Implementation and Design

We set the A* Pathfinding Local Avoidance controller to update the agents at a speed of 20 frames per second and we are using the gradient decent algorithm to find the optimal velocity for the agents. The most challenging part of implementing the virtual agents was getting them to navigate the environment as realistic groups based on Moussaids three group formations. In real life scenarios Moussaid observed the line-abreast formation in low density crowds. The v-like formation is observed when the density of the crowd would be described as moderate, and the river-like formation is observed in high density crowds (Figure 2-1) [7].

A* Pathfindings Local Avoidance implementation does not support grouping. Our solution to force this behaviour on the agents is to create what I refer to as a leader agent. The leader agent has a waypoint destination and 3 waypoints connected to it which are the waypoints for each agent in the group. The leader agents are set to avoid each other while ignoring the actual virtual agents. It was theorized that the leader agent would steer each agent group around each other (Figure 3-7).

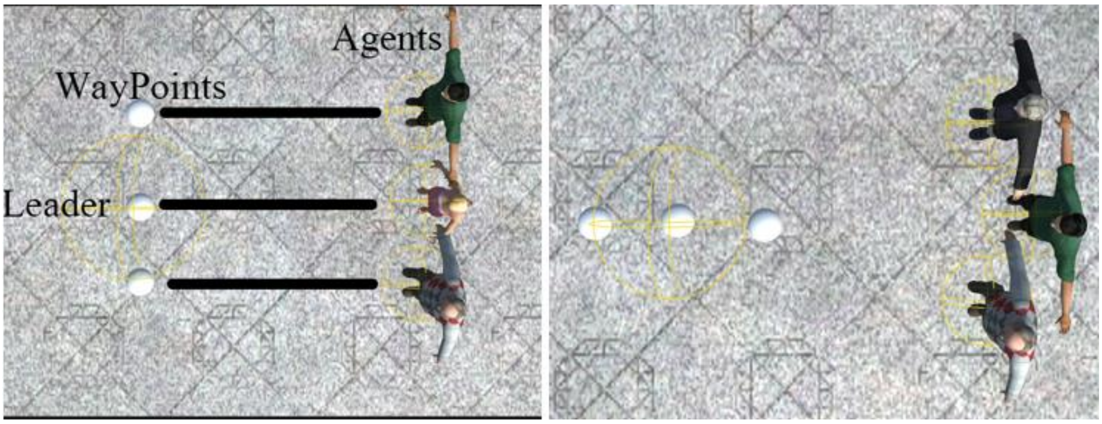

Figure 3-7: Solution to force grouping behaviour.

Initially the distance between the waypoints and the agents was only 1 unit in length. This allowed the agents to avoid each other as a group quit effectively as they navigated based on the leader agents decisions (Figure 3-8).

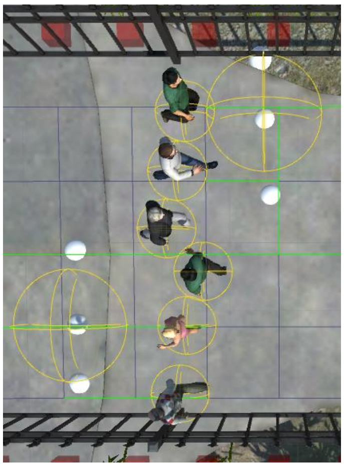

Figure 3-8: Avoiding other agent groups without breaking formation

However, there are some issues with this particular implementation. If the participant's avatar is moving- which they will be there is simply not enough time for the virtual agents to make any avoidance around the participant's avatar as their way point destination is too close.(Figure 3-9).

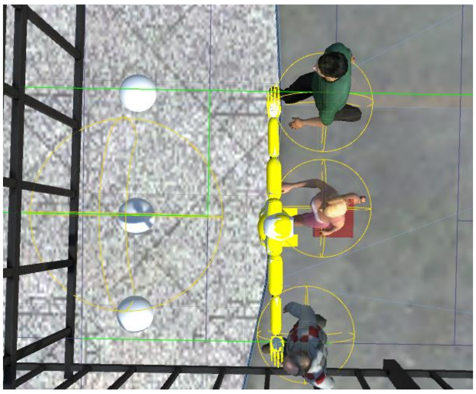

Figure 3-9: The virtual agents do not have enough time to navigate around the player's avatar, the red box is the dynamic obstacle location of the avatar.

The decision to increase the distance was made to allow the virtual agents to "see" and make some avoidance around the participants if necessary. We found it to be more important for the integrity of the experiments to ensure that the agents would be able to navigate around the participant if they had to. This was more important than the agents being able to navigate around each other as group because in real life collision avoidance situations between pedestrians it is a collaborative effort to not collide with each other. It has been shown that between 2 pedestrian walkers, collision avoidance is a collaborative, but role dependant in nature. The results show that on average one of the pedestrians are giving way to the other by contributing 60% of the effort to the collision avoidance, while the other contributes on average 40% of effort to the avoidance. The percentage of effort was calculated by comparing the computed principle of minimum energy and comparing that to the actual trajectories and time of completion between the two walkers [13].

Unfortunately, increasing the distance left the agents with some undesirable behaviour when avoiding each other- which is highlighted in Figure 3-10, which shows the grouped agents stopped being able to navigate around other oncoming agent groups as a whole unit. However, it is nice to see on the left of Figure 3-10, where the group moving to the left adopts the v-like formation as they avoid through the group moving towards the right. The virtual agents are now able to see and navigate around the participant's avatar if they have to. The virtual agents are notified of the participant's avatars location every 0.1seconds, by calling a function to update the pathfinding graph for the agents navigation.

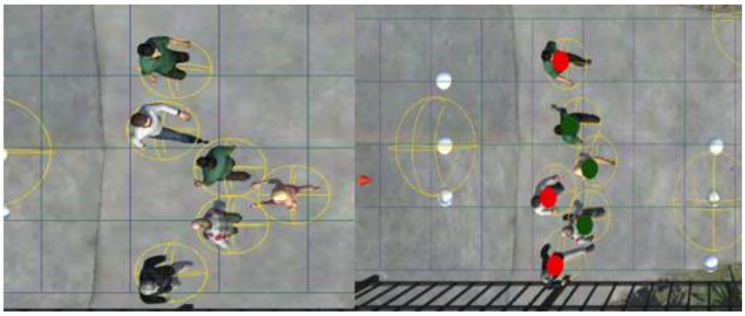

Figure 3-10: Agents no longer able to avoid around the oncoming agent groups.

We initially designed the virtual agents to mimic the walking speed of real pedestrian groups based on research by Moussaid [7]. However, during testing the speed felt too fast, possibly due to the distance compression from viewing the virtual world through a digital display [15, 16, 17]. Additionally, walking speed is reduced while inside a virtual reality world [25]. Therefore, it makes sense that we would not be able to use real world walking speeds for a virtual agents. We reduced the speed of the back facing virtual agents in the low density tests by 33% to try and force the participants to either go through or around the back facing agents.

3.2.3 Stereoscopic Display and Head Tracking.

For the stereoscopic display we are using the camera rig from the Unity3D Google Cardboard integration package [36]. The Google Cardboard stereoscopic display works very well in the Unity3D editor. However, when the Unity3D project was built it was missing the distortion correction (Figure 3-11). Due to time constraints we were unable to figure out why this was happening. When the distortion correction is missing the objects in the scene appear slightly distorted as, the image on the bottom shows the shapes and environment appearing to be slightly longer than they actually are if we refer to the non- distorted image on the top. It is expected that the lack of distortion correction will add some bias to the experiments conducted- which is discussed in chapter 4.2.3.2.

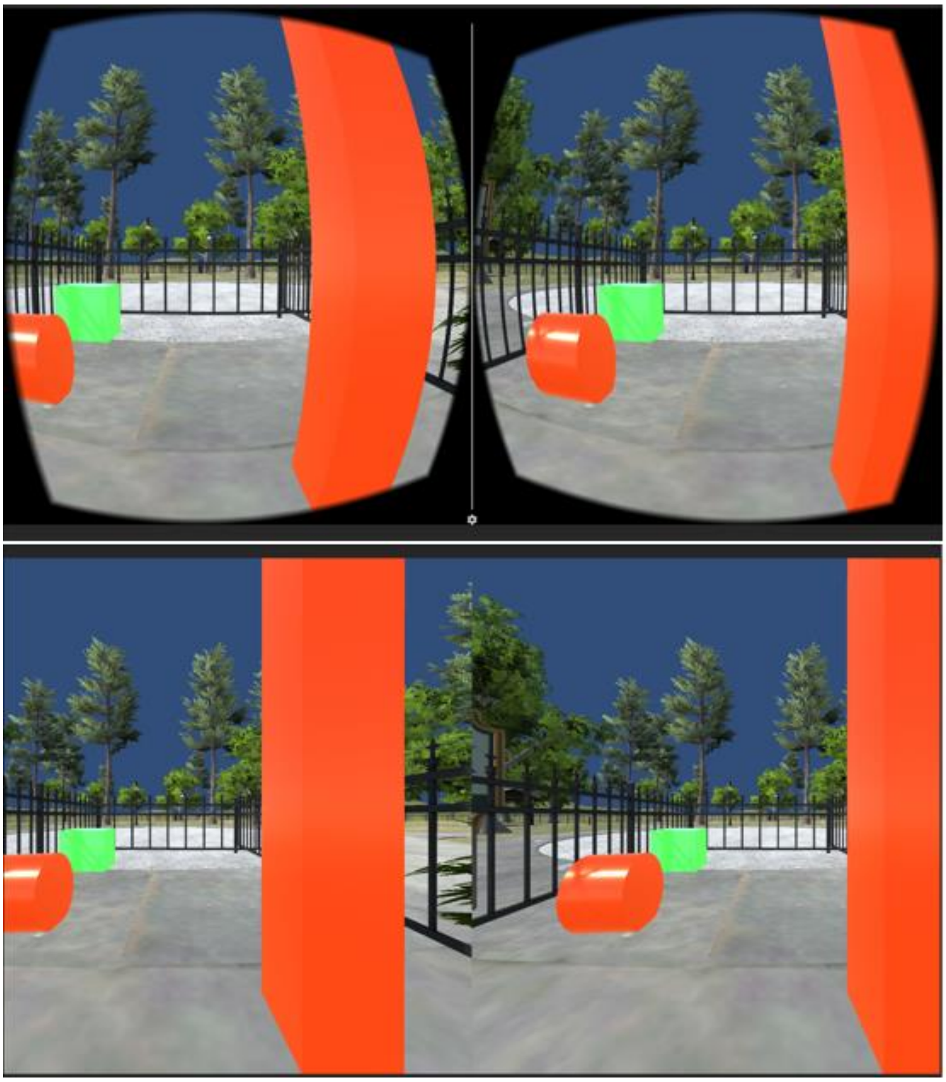

Figure 3-11: Image on the top has distortion correction and is what is seen in the Unity3D editor, the image on the bottom does not have distortion correction and is what the project was built as.

The head tracking of the virtual reality system is being performed by the head mounted Neuron from the Perception Neuron kit. The stereoscopic camera rig's position and rotation is equal to that of the Perception Neuron avatars head position and rotation. The head mounted Neuron is very sensitive- so while walking the user would experience a fair amount of roll for each step they took; about 4-6 degrees of roll (Figure 3-13)- making the whole virtual reality world wobble every time the participant moved their head. It should be noted that the developers of the Perception Neuron kit do not recommend that the head rotation data from the Perception Neuron system be used for head tracking, the reason for this would be due to the fact that you need to smooth the output values- as the raw output is too sensitive for comfortable head tracking [31]. However, there was no easily and quickly implementable alternative, in the time frame that we had. The yaw and pitch of head tracking felt fine. We attempted to smooth the output from the head mounted Neuron on the Z axis, but nothing we tried was able to remove the wobble completely.   Due to this immersion breaking behaviour we decided to stop updating the cameras position on the Z axis. We do not feel that doing so will have any effect on the results at all as there is no reason during any of the experiments for the participant to rotate their head along the Z axis.

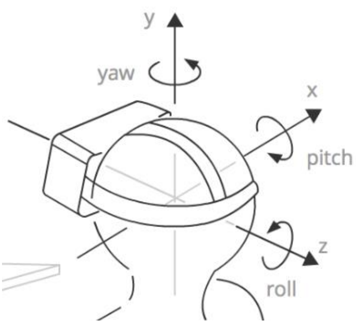

Figure 3-12: Head Mounted display yaw, roll and pitch. We had to remove the roll ability.

3.2.4 Perception Neuron Integration

Perception Neuron was integrated into Unity3D by using the Unity3D integration package (V 0.25) supplied by Perception Neuron. The perception Neuron integration requires you to create a new layer called “body” and remove the ability for the “body” layer to collide with itself in the settings. It was then a matter of dragging and dropping the Perception Neuron avatar prefab into the unity3D scene. The positional and rotation data representing the user’s current position and rotation is being broadcast locally from the Axis Neuron software as binary float values, in the BVH format via a TCP connection to ensure accurate motion tracking. The rotation and positional data for each of the limbs and body parts are then used to rotate and move the avatars limbs and body parts in Unity3D.

3.3 Virtual Reality Framework

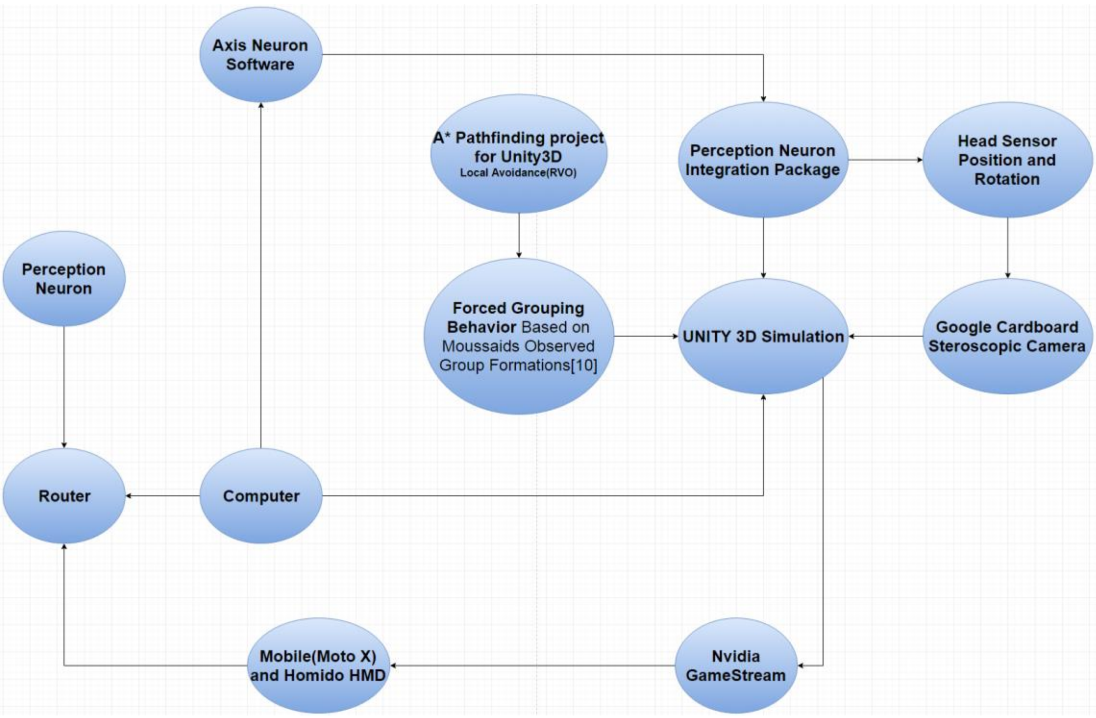

Figure 3-13: Complete virtual reality Framework.

4 Experiment Design and Methodology

In the Previous chapter we discussed the Implementation of the hardware and software components required to build our experimental virtual reality framework. In this chapter we are taking our proposed virtual reality implementation and using it for the investigation of individual pedestrian's navigation decisions when moving through crowds.

Phase 1: Testing the spatial drift of the perception neuron suit to ensure the participants won't drift into any walls.

Phase 2: Using Virtual reality in the form of a motion capture suit and head mounted display to study how an individual pedestrian will navigate through virtual crowds.

4.1 Phase 1: Testing the Spatial Drift over time of the Perception Neuron Suit.

Before we can perform any experiments investigating how an individual navigates through a crowd using our virtual reality framework we first need to benchmark the spatial drift of the Perception Neuron inertial motion unit based motion capture suit. Due to inertial motion sensors susceptibility to drift over time it is imperative to know exactly how much the Perception Neuron suit drifts overtime when it is being used as the avatar controller for a 3D virtual reality simulation or game with a head mounted display.

When designing the 3D environment we need to take into account the drift that the suit creates when setting the environments dimensions. The dimensions of the virtual world need to be x metres less than the real world area the suit is being used in because we don't want the user to drift into a wall. The purpose of this experiment is to determine what x should be for the designing of safe 3D environments for the Perception Neuron suit to be used in.

4.1.1 Framework and Design

During this experiment I am moving back and forth between location A and B in the real world for 1,2,3,4,5,6,7 and 8 minutes. I am measuring the amount of spatial drift that the virtual avatar in Unity3D is experiencing over time. This experiment was performed 10 times. However, there was some calibration issues with the suit which lead to two separate data sets:

1. Good motion capture data (6 times) -where after the 8 minutes of continuous use the motion capture of the suit is still decent.
2. Bad motion capture data (4 times) - where after 8 minutes of continuous use the motion capture of suit is unacceptable.

The reason for the suits unacceptable motion capture after 8 minutes in some cases is unknown. Although, if I had to guess I would say it is due to a combination of variables; my personal error when performing the calibration poses, or the sensors moving positions due to the straps on my body moving slightly out of position. Regardless of the reasons for the bad motion capture, the two datasets will be interesting to compare; as there is always the chance of participants in a virtual reality study being incorrectly calibrated.

From this experiment we hope to establish the amount that the suit drifts after continuous use for 1,2,3,4,5,6,7 and 8 minutes and if the amount of spatial drift increases linearly or exponentially over time.

The experiment setup (Figure 4-1) for the experiment consists of wirelessly connecting the Perception Neuron suit with the Axis Neuron software. The Perception Neuron suit is paired with the Unity3D simulation by using the Unity3D integration package developed by the Perception Neuron developers. Additionally, a wireless mouse is used to record the virtual avatars position inside Unity3D when the wearer of the suit reaches the location A or the location B in the real world.

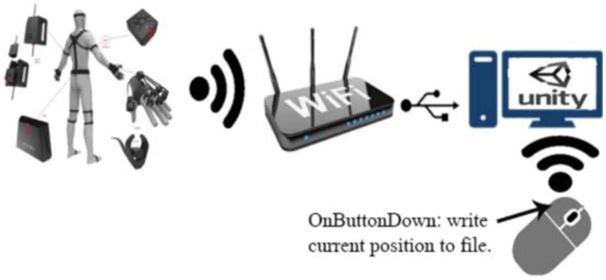

Figure 4-1: Spatial drift experiment equipment setup.

The real-world test area had two chairs placed 5 metres apart to act as point A and point B. It should be noted that the points (chairs) are placed 20cm passed the 5 metre and 0 metre mark. This allows us to move roughly 5 metres in between the two points without running into the points (chairs). However, there will be a deviation of up to 20cm passed the 0 or 5 metre marks respectively. Furthermore, the points (chairs) are placed directly in line with each other. The real-life test area is reflected in Unity3D where each unit is equal to 1 metre. Therefore, point A and point B in Unity3d are placed 5 units apart (Figure 4-2).

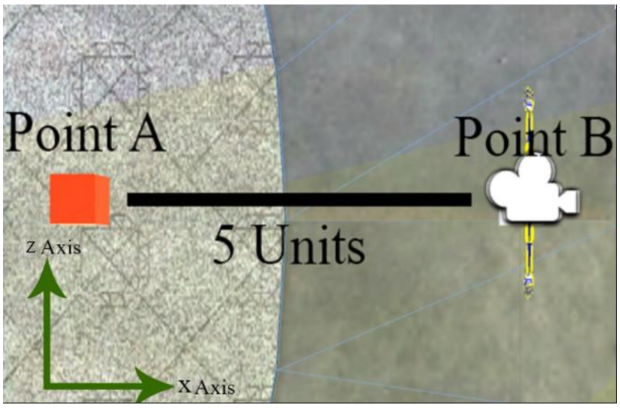

Figure 4-2: The points in unity are 5 units (metres) apart.

4.1.1.1 The data to be recorded includes:

- X, Z Coordinates of the avatar in Unity3D.
- The time it took to go from point A to point B.

4.1.1.2 Procedure:

1. Strap on the Perception Neuron suit.
2. Connect to the suit to the Axis Neuron software.
3. Set the skeletons height to 180cm in Axis Neuron software.
4. Run calibration poses on the starting location.
5. Ensure the suit is providing smooth leg motion (this drives the motion of the avatar so it is very important).
6. Start experiment simulation
7. Walk for 8 minutes in between location A and B.
8. Check and note if the skeleton in axis neuron is still giving acceptable data.
9. Disconnect the suit.
10. Repeat steps 2 to 8, 10 times.

4.1.2 Results:

4.1.2.1 Limitations of data collected

The biggest limitation of the data that has been collected from this experiment is the positional data of the suit not being able to be captured at the exact minutes. The reason for this is because it is not possible for me-being a human to sync my movements to land on either point A or point B for each minute perfectly. Additionally, where the timescale of some of the charts is in minutes the positional data for points A and B are captured on average about 11 seconds apart as shown in Figure 4-3.

Point	X	Z	Seconds	Minutes data point
Point A	135.1433	129.4691	49.8138	1
Point B	140.1613	130.4373	60.78491	1

Figure 4-3: Points not able to be captured on the exact minutes.

4.1.2.2 Outliers

Figure 4-4 highlights the outliers and the average drift on each axis for both point A and B from 8 minutes of continuous use. The highest outlier amount of drift experienced by the avatar was 5.56m on the Z axis in the bad dataset, while the good datasets highest outlier is 2.3726m on the X axis. The cause of these outliers is un-known, they could be problems with calibration, the Neurons on the body moving out of position, or even slight network lag or dropouts. Regardless of the reasons why they are here, they do need to be taken into account when determining safe dimensions for our virtual reality environment, because they occurred once and could occur again. However, if we could ignore the presence of the outliers and look only at the average amount of drift from each of the tests conducted the amount of drift is very impressive. The good motion capture dataset had an average drift from both points of 0.99m (X axis) and 0.96m (Z axis) from 8 minutes continuous use. Whereas, the bad motion capture dataset experienced considerably more drift with 1.76m (X axis) and 2.36m (Z axis).

Good Mocap Average Amount of Drift after 8 Minutes		
	X	Z
Average Both Points	0.996967	0.962192
Average Point A	1.020483	0.895417
Average point B	0.97345	1.028967
Bad Mocap Average Amount of Drift after 8 Minutes		
	X	Z
Average Both Points	1.76535	2.368888
Average Point A	1.937225	2.43225
Average point B	1.593475	2.305525

	Good X	Good Z	Bad X	Bad Z
Test1: Point A	0.4086	1.2083	1.9042	5.5627
Test1: Point B	0.4655	1.249	2.2332	5.447
Test2: Point A	0.6915	1.0715	3.4367	1.8552
Test2: Point B	0.5673	1.2048	1.5335	0.9843
Test3: Point A	0.1236	0.8962	1.276	0.8165
Test3: Point B	0.0615	1.1295	1.3278	1.1487
Test4: Point A	0.7676	0.8647	1.132	1.4946
Test4: Point B	0.922	1.5678	1.2794	1.6421
Test5: Point A	2.3726	0.0218		
Test5: Point B	2.2555	0.1788		
Test6: Point A	1.759	1.31		
Test6: Point B	1.5689	0.8439		

Figure 4-4: The accumulated amount of drift over 8 minutes for both the good motion capture data set and the bad motion capture dataset.

4.1.2.3 Incorrect angle of motion

Unfortunately, all the data points I collected have an incorrect angle of motion (Figure 4-5). This is bad because in the real world we were walking in a straight line. The angle of motion in real life could be described as very close to 0 degrees. The incorrect angle of motion is caused by the avatar being rotated at the wrong degrees. This is a significant problem for the designing of safe dimensions for the virtual environment. If you travel 5 metres in a straight line and the avatar has an incorrect angle of motion on 9.6 degrees the avatars position in the virtual environment will be offset by 0.84 metres on the Z axis, and if you travel 15 metres the avatar will be offset by 2.53 metres. The reason for why the incorrect angle of motion is occurring is unknown. However, the fact that it is occurring does need to be taken into consideration when determining safe dimensions of the virtual reality environment.

Bad Mocap Average Angles of Motion			
	Final 1 Minute	Final 8 Minute	Starting
Test 1	4.296324729	5.009996922	4.673341089
Test 2	2.841007596	4.668684721	2.90248235
Test 3	12.06877992	12.06312678	12.18631084
Test 4	12.82214557	12.77901234	13.15148932
Average	8.007064454	8.63020519	8.228405901
Difference Between Final 1		0.623140736	0.221341447

Good Mocap Average Angles of Motion			
	Final 1 Minute	Final 8 Minute	Starting
Test 1	10.23891858	10.38844672	10.50671513
Test 2	13.51746284	13.40073982	13.75092209
Test 3	9.25196633	9.128471555	9.462883847
Test 4	5.015062802	5.136541397	5.296126957
Test 5	10.96873971	11.19017043	10.94850562
Test 6	8.499118556	8.576289561	8.274282741
Average	9.581878138	9.636776581	9.706572731
Difference Between Final 1		0.054898443	0.124694593

Figure 4-5: The angle that the avatar was walking at.

4.1.2.4 Visualisation of the Drift (Metres) Over Time (Minutes)

Figure 4-6 to Figure 4-9 display the amount of drift in metres for each minute interval. It should be noted that the graphs are showing the drift along each axis(X and Z) for each of the points. The results appear to be very sporadic. You can notice that some of the tests for both point A and B are experiencing massive increased in drift over a minute period. It is unclear what is causing the massive increases in the drift. In some of the case they do not continue to increase at the same magnitude, while in others they do. The unexpected increases are very perplexing, we can give a few explanations as to why they are occurring but we will not be able to prove or disproved them until more rigours experiments are performed in future work. We theorize that there are two things that could be creating such increases, one: the Perception Neurons “drift correction” had a heart attack, causing the legs and/or feet to become bent, thus moving more forward then they were previously; or two: it is due to a network dropout or lag.

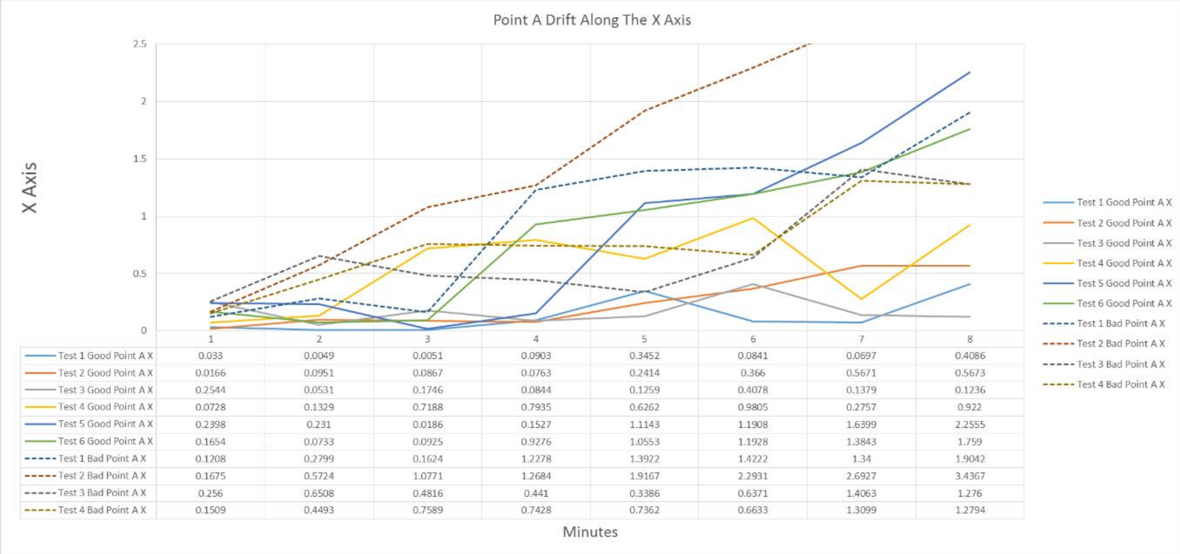

	1	2	3	4	5	6	7	8
Test 1 Good Point A X	0.033	0.0049	0.0051	0.0903	0.3452	0.0841	0.0697	0.4086
Test 2 Good Point A X	0.0166	0.0951	0.0867	0.0763	0.2414	0.366	0.5671	0.5673
Test 3 Good Point A X	0.2544	0.0531	0.1746	0.0844	0.1259	0.4078	0.1379	0.1236
Test 4 Good Point A X	0.0728	0.1329	0.7188	0.7935	0.6262	0.9805	0.2757	0.922
Test 5 Good Point A X	0.2398	0.231	0.0186	0.1527	1.1143	1.1908	1.6399	2.2555
Test 6 Good Point A X	0.1654	0.0733	0.0925	0.9276	1.0553	1.1928	1.3843	1.759
Test 1 Bad Point A X	0.1208	0.2799	0.1624	1.2278	1.3922	1.4222	1.34	1.9042
Test 2 Bad Point A X	0.1675	0.5724	1.0771	1.2684	1.9167	2.2931	2.6927	3.4367
Test 3 Bad Point A X	0.256	0.6508	0.4816	0.441	0.3386	0.6371	1.4063	1.276
Test 4 Bad Point A X	0.1509	0.4493	0.7589	0.7428	0.7362	0.6633	1.3099	1.2794

Figure 4-6: Point A, amount of deviation from the starting location along the X axis for each minute.

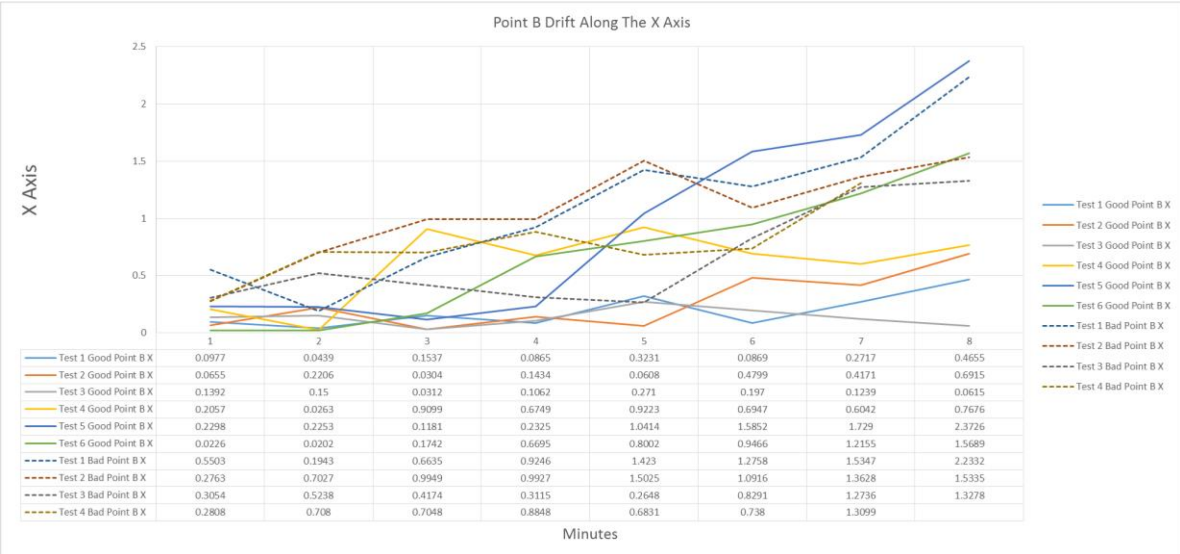

	1	2	3	4	5	6	7	8
Test 1 Good Point B X	0.0977	0.0439	0.1537	0.0865	0.3231	0.0869	0.2717	0.4655
Test 2 Good Point B X	0.0655	0.2206	0.0304	0.1434	0.0608	0.4799	0.4171	0.6915
Test 3 Good Point B X	0.1392	0.15	0.0312	0.1062	0.271	0.197	0.1239	0.0615
Test 4 Good Point B X	0.2057	0.0263	0.9099	0.6749	0.9223	0.6947	0.6042	0.7676
Test 5 Good Point B X	0.2298	0.2253	0.1181	0.2325	1.0414	1.5852	1.729	2.3726
Test 6 Good Point B X	0.0226	0.0202	0.1742	0.6695	0.8002	0.9466	1.2155	1.5689
Test 1 Bad Point B X	0.5503	0.1943	0.6635	0.9246	1.423	1.2758	1.5347	2.2332
Test 2 Bad Point B X	0.2763	0.7027	0.9949	0.9927	1.5025	1.0916	1.3628	1.5335
Test 3 Bad Point B X	0.3054	0.5238	0.4174	0.3115	0.2648	0.8291	1.2736	1.3278
Test 4 Bad Point B X	0.2808	0.708	0.7048	0.8848	0.6831	0.738	1.3099	

Figure 4-7: Point B, amount of deviation from the starting location along the X axis for each minute.

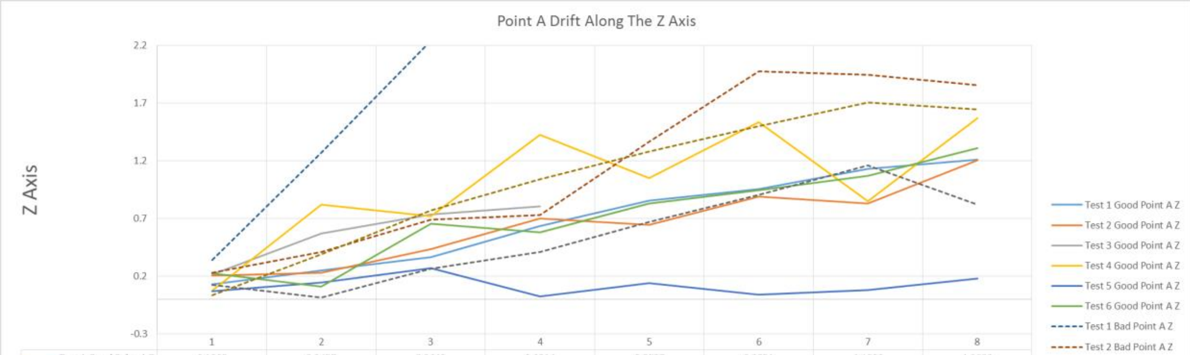

	1	2	3	4	5	6	7	8
Test 1 Good Point A Z	0.1269	0.2457	0.3642	0.6314	0.8537	0.9551	1.1289	1.2083
Test 2 Good Point A Z	0.2049	0.2263	0.434	0.698	0.6458	0.8872	0.8288	1.2048
Test 3 Good Point A Z	0.2127	0.569	0.7333	0.8018				
Test 4 Good Point A Z	0.0729	0.8173	0.7188	1.4239	1.0484	1.5358	0.8468	1.5678
Test 5 Good Point A Z	0.0676	0.1437	0.2693	0.025	0.1389	0.0401	0.0793	0.1788
Test 6 Good Point A Z	0.2243	0.1081	0.6521	0.5804	0.8282	0.9448	1.0688	1.31
Test 1 Bad Point A Z	0.337	1.2699	2.24	2.7024	3.5684	4.1576	4.7123	5.5627
Test 2 Bad Point A Z	0.2292	0.4064	0.6902	0.7302	1.3622	1.9754	1.9459	1.8552
Test 3 Bad Point A Z	0.1223	0.0106	0.2627	0.4091	0.6661	0.9046	1.1568	0.8165
Test 4 Bad Point A Z	0.034	0.3892	0.7688	1.04	1.2778	1.4988	1.7044	1.6421

Minutes

Figure 4-8: Point A, amount of deviation from the starting location along the Z axis for each minute.

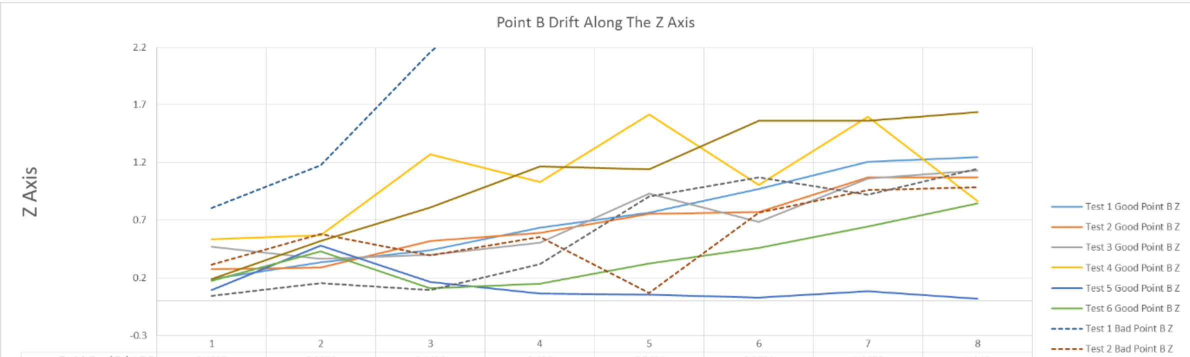

	1	2	3	4	5	6	7	8
Test 1 Good Point B Z	0.1887	0.3372	0.4426	0.636	0.7684	0.9734	1.2079	1.249
Test 2 Good Point B Z	0.2732	0.2926	0.5209	0.5914	0.7539	0.7725	1.0724	1.0715
Test 3 Good Point B Z	0.4727	0.3667	0.4017	0.5068	0.9324	0.6849	1.0611	1.1295
Test 4 Good Point B Z	0.5337	0.5711	1.2739	1.0293	1.6184	1.0078	1.5981	0.8647
Test 5 Good Point B Z	0.0968	0.4812	0.1678	0.0636	0.0554	0.0289	0.0858	0.0218
Test 6 Good Point B Z	0.1757	0.4301	0.1084	0.1485	0.3274	0.4618	0.6463	0.8439
Test 1 Bad Point B Z	0.8059	1.1746	2.1561	2.9458	3.5437	4.3724	5.0517	5.447
Test 2 Bad Point B Z	0.317	0.5791	0.3948	0.5565	0.0715	0.768	0.9599	0.9843
Test 3 Bad Point B Z	0.0467	0.1578	0.094	0.3192	0.9076	1.0693	0.9204	1.1487
Test 4 Bad Point B Z	0.1918	0.5195	0.8129	1.1672	1.1436	1.5643	1.564	1.6353

Minutes

Figure 4-9: Point B, amount of deviation from the starting location along the Z axis for each minute.

4.1.2.5 Statistical Analysis of Drift (Metres) Over Time (Minutes)

A two sample t- test was performed on the data to determine if the population means of point A and B are the same. We do not know the variance of the data, so we assume them to be unequal. Our alpha value is 0.05, this means that we can either reject or accept the null hypothesis with a confidence level of 95%. The null hypothesis in this case is that the means of the data are not significantly different, whereas the alternative hypothesis states that the means of the data are significantly different. The null hypothesis is accepted if the P value is higher than the alpha (0.05), if it is less the alternative hypothesis is accepted.

Good Data Set t-Test: Two-Sample Assuming Unequal Variance, Between Each Identical Axis of Point A and B								
Calculation	Test 1: A:X, B:X	Test 1 A:Z, B:Z	Test 2 A:X, B:X	Test 2: A:Z, B: Z	Test 3 A:X, B:X	Test 3: A:Z, B: Z	Test 4 A:X, B:X	Test 4: A:Z, B: Z
df	16	16	14	14	12	13	14	13
t Stat	-0.908523526	-0.203030184	-0.099826234	-0.167462768	0.732170422	0.055633815	-0.208160228	-0.251637902
P(T<=t) two-tail	0.377083612	0.841670911	0.921897681	0.869400834	0.478121423	0.95647948	0.838101741	0.805255127
t Critical two-tail	2.119905299	2.119905299	2.144786688	2.144786688	2.17881283	2.160368656	2.144786688	2.160368656
	Test 5 A:X, B:X	Test 5: A:Z, B: Z	Test 6 A:X, B:X	Test 6: A:Z, B: Z				
df	14	11	14	12				
t Stat	-0.204379336	-0.120777712	0.505278161	1.879498009				
P(T<=t) two-tail	0.840998427	0.906045016	0.62122434	0.08467079				
t Critical two-tail	2.144786688	2.20098516	2.144786688	2.17881283				

Figure 4-10: Two- sample t-test, assuming unequal variance between each identical axis of point A and B for each test in the good motion capture data set. The green highlight shows that the P value being higher than the alpha (0.05). Therefore, we accept the null hypothesis.

Bad Data Set t-Test: Two-Sample Assuming Unequal Variance, Between Each Identical Axis of Point A and B								
Calculation	Test 1: A:X, B:X	Test 1 A:Z, B:Z	Test 2: A:X, B:X	Test 2 A:Z, B:Z	Test 3: A:X, B:X	Test 3 A:Z, B:Z	Test 4: A:X, B:X	Test 4 A:Z, B:Z
df	14	14	9	10	14	14	12	14
t Stat	-0.355149537	-0.135337601	1.480279652	-0.135337601	0.135495329	-0.179082163	-0.626768792	-0.106864435
P(T<=t) two-tail	0.727771109	0.894271573	0.172931926	0.067908647	0.894149158	0.860439045	0.542551292	0.916412788
t Critical two-tail	2.144786688	2.144786688	2.262157163	2.228138852	2.144786688	2.144786688	2.17881283	2.144786688

Figure 4-11: Two- sample t-test, assuming unequal variance between each identical axis of point A and B for each test in the bad motion capture data set. The green highlight shows that the P value being higher than the alpha (0.05). Therefore, we accept the null hypothesis.

Good Data Set t-Test: Two-Sample Assuming Unequal Variance, Between Each Axis of opposite axis for Point A						
Calculation	Test 1: A:X, A:Z	Test 2: A:X, A:Z	Test 3: A:X, A:Z	Test 4: A:X, A:Z	Test 5: A:X, A:Z	Test 6: A:X, A:Z
df	10	12	10	13	7	12
t Stat	-4.077042239	-2.689975522	-5.825909154	-2.005500304	2.528354862	0.431437389
P(T<=t) two-tail	0.002224897	0.019670736	0.000166974	0.066185001	0.03932737	0.673799696
t Critical two-tail	2.228138852	2.17881283	2.228138852	2.160368656	2.364624252	2.17881283

Figure 4-12: Two- sample t-test, assuming unequal variance between each opposite axis of point A for each test in the good motion capture data set. The green highlight shows that the P value is higher than the alpha (0.05). Therefore, we accept the null hypothesis. Whereas, the yellow highlight shows the P value being smaller than the alpha (0.05). Therefore, we reject the null hypothesis.

Figure 4-11 and Figure 4-12 show that there is no significant difference between the amount of drift observed from point A and point B on the identical axis's of each test. Due to the identical axis's of point A and B having no significant difference in population mean we ran a second t-test comparing the opposite axis's for only point A (Figure 4-13). The results from running the t-test on the opposite axis's shows that there is the potential for there to be a significant difference between the X and Z axis's for the majority of the tests. The reason is unclear- but it is possible that it is due to some kind of difference in the calibration of the sensors, and as such needs to be taken into consideration when designing the dimensions of the virtual environment as the results show there can be a significant difference between the X and Z axis's.

4.1.3 Discussion and recommendations of virtual environment dimensions.

In chapter 4.1.2.5 we discovered that there is a significant difference in the population means of the drift on the X axis and Z axis. This means that when designing the environment we can assume that the drift on X and Z axis will experience significantly different amounts of drift. If we refer to chapter 4.1.2.2- Figure 4-4 we can corroborate the t-test values by visually looking at the difference in drift on each axis. Figure 4-4 also shows that there is no consistent pattern of less drift occurring on the X axis when compared to the Z or vice versa. This means that we will not be able to set the dimensions of the virtual world to be based on the drift that occurred on each axis, instead we will have to assume that the highest amount of drift; 5.56m from the bad motion capture data set on the Z axis from 8 minutes of continuous use, will also be able to occur on the X axis. Additionally, we need to consider the impact that the incorrect angle of motion observed in chapter 4.1.2.3 will have on the environment- as it is causing an additional positional offset of the avatar on the Z axis. The highest angle of motion observed was 13.7 degrees, while the lowest was 2.8 degrees, with an average of about 9.6 degrees. When calculating the safe dimensions for the virtual environment we will have to assume that the worst case scenarios from our obtained results.

Formulas for the Offset of the Drift.

$$X\ axis\ drift\ per\ minute = \frac{Highest\ Total\ drift\ (m)}{Time\ period\ (min)}$$

Equation 4-1: Where highest total drift = 5.56m and time period = 8 minutes

Therefore, for every minute of use we have to account for 0.695m of drift on the X axis.

$$Z\ axis\ drift\ per\ minute = \frac{Highest\ Total\ drift\ (m)}{Time\ period\ (min)} + (Tan(\theta) * Traveled\ distance)$$

Equation 4-2: Where highest total drift = 5.56m, time period = 8 minutes, θ is the highest angle of motion = 13.7 and travel distance = 15m.

Therefore, for every minute of use we have to account for 0.695*(minutes) + 3.65m on the Z axis.

> *In hindsight, it should be noted that you technically only need to account for the 3.65m on one of the Z axis sides, if you know the direction the angle of motion is offsetting the avatars position on the Z axis in relation to the users real life movement. In our case the avatar was only being offset on the right hand side of the participant and on the positive side of the Z axis. Therefore, we only needed to take the angle of motion into account for the positive side of the Z axis.*

4.2 Phase 2: Virtual Reality Experiment, Investigating How an Individual Navigates through Crowds.

Our previous experiment investigated exactly how much we would have to offset the dimensions of the virtual world for our virtual reality experiment to be safe.

This experiment aims to investigate how individual pedestrians navigate through crowds of realistic group formations with different visual appearances. To that end we will also validate our completely wireless virtual reality framework by using it in this experiment.

4.2.1 Framework and Experiment Design

The hardware and software framework for this experiment has been outlined in chapter 3.

4.2.1.1 Virtual Environment and Real-World Testing Area

Using the formulae from chapter 4.1.3 we are able to determine safe dimensions for the virtual environment. The real world testing area that we have to work with is 10 metres in width and 19 metres in length. Additionally, the experiment is expected to take less than 4 minutes to complete, the participants virtual avatar's position will be reset at the ~2 minute mark. This means that the virtual world needs to be at least 1.39 units smaller on each side of the X axis, and at least 5.04 units smaller on each side of the Z axis. Factoring these dimensions into the design of the virtual world left with a virtual world that was 15 units long on the X axis and 5 units wide on the Z axis. (Figure 4-13) Furthermore, the participants began the experiment in the middle of both the virtual world and real world on the Z axis (width), and where 2 metres/units away from the end of the X axis (length). This was especially important to allow for there to be ~ 5 metres of real-world space on each width side to prevent the incorrect angle of motion from making the participants walk out of the real world safe zone (red rectangle)

The setting of the virtual world was not designed to be of any significance for this experiment; it is an outside footpath area whose boundaries are fenced off to let the participants know they cannot go out of the virtual bounds.

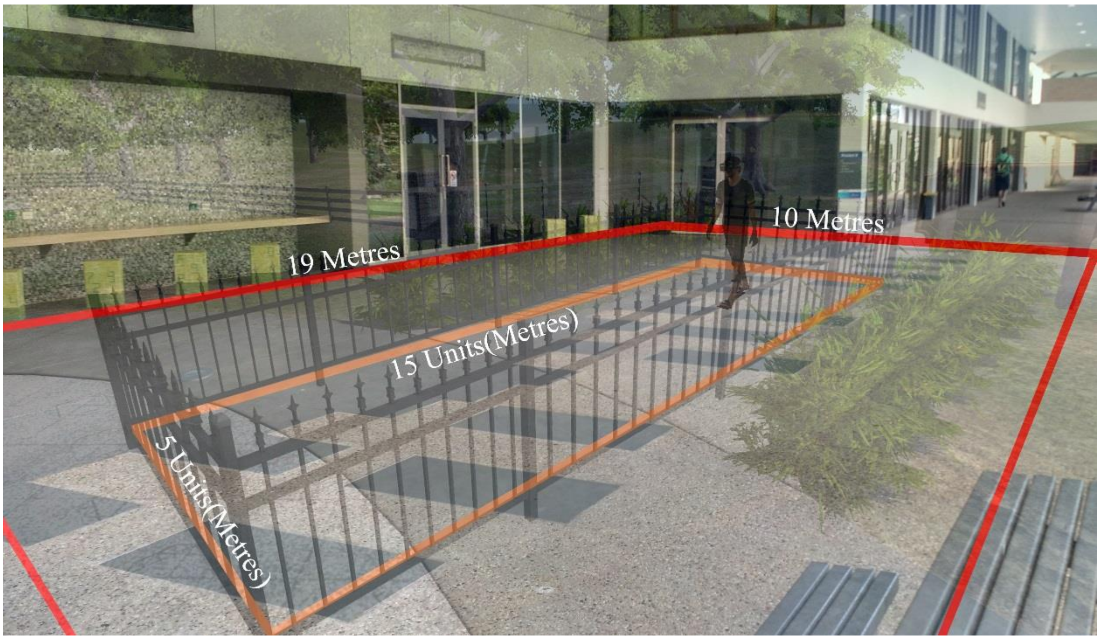

Figure 4-13: Virtual environment and real-world testing area overlay.

4.2.1.2 Experiment Scenarios

In this experiment the participants are tasked with walking to easily visible cubes on opposite sides of the virtual environment. There are two separate experiment tests the normal appearance test where the virtual people appear as normal people and the social appearance test where the virtual people have an easily distinguishable social connection (soldiers) (Figure 4-14)

Figure 4-14: On the left is the normal appearance test models, and on the right is the social appearance test models.

Figure 4-15 shows the different variables being tested during the 4 experiment tests. The first experiment to be run will be the normal appearance tests. When the participant is comfortable inside the virtual environment they are able to interact with an object in the virtual world to begin the experiment. This triggers the first test to begin where the participant is tasked with navigating the virtual crowd to reach and interact with an easily visible object at the end of the virtual world boundary- which will trigger the second test. It should be noted that after the first and second test the participant's virtual avatars position will be reset to remove the accumulated drifting errors before performing test three and four; which has the same process as test one and two.

The Variables That are Tested.			
Test Number	**Gaze behaviour**	**Appearance**	**Density of Crowd**
1	Back and front Facing	Normal	Low
2	Back and front Facing	Normal	Moderate-High
3	Back and front Facing	Social-link	Low
4	Back and front Facing	Social-link	Moderate-High

Figure 4-15: Shows the different variables being tested during the Experiment.

4.2.1.3 Data Collection

The data to be collected during the experiment is quite extensive and is being written to .CSV files every 0.1 seconds.

- Positional and rotational(X, Y, Z) of each of the bones of the participant's avatars Skelton.
- Participant's avatars head position and rotation (X, Y, Z).
- Every virtual agent's position(X, Y, Z), Group ID, Agent ID and direction of movement(X+ or X-).

We are also collecting qualitative data in the form of surveys and questionnaires that are to be filled out after the experiment.

4.2.2 Data Analysis

We had a total of 10 people (1 woman and 9 men) volunteer to take part in our virtual reality experiment investigating how an individual navigates though a virtual crowd. However only 9/10 participants successfully completed the experiment tasks. The participants where aged between 21 and 45 with an average combined age of 26 and only 50% had used a virtual reality head mounted display before taking part in our virtual reality study. However, on a scale of 1 to 7 where 7 is very good the participants scored an average of 5.2 for being "very good" at 3D videogames.

Figure 4-16 shows the basic visualisation of the data and includes, the participant's velocity and head rotation. Due to time constraints we were unable to visualise the participants avatars bone data.

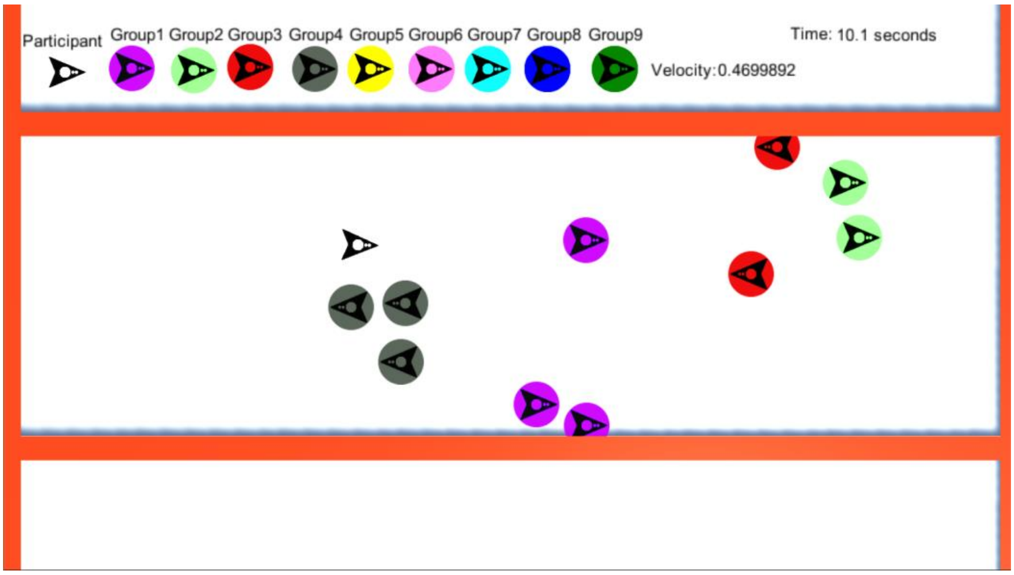

Figure 4-16: Basic Visualisation of the data.

The visualisation was observed visually to determine the navigational decisions and strategies of the participants. We collected the following data from these observations:

- Distance of avoidance (Going around).
- Distance of gap (Going through).
- Velocity that the participant is traveling when the decision occurs,
- The pitch(X) and yaw(Y) rotation of the participants head.

4.2.3 Results

We used a true/false model for visualising the navigation decisions of our participants. Where 1= they went around/through and 0 = they didn't go around/through. Two sample t-Test's assuming unequal variances with an alpha level of 0.05 where run on our collected qualitative data to determine if the decision to go through or around the virtual agent groups is statistically significant.

4.2.3.1 Limitations

From reviewing the visualisation of each of the participants navigating through the virtual crowds we found that the majority of the participant's did not begin moving towards the goal object as soon as the experiment was started. The simulation was designed with the assumption that the participants would begin moving as soon as the virtual agents where spawned into the scene. Unfortunately, this means that the majority of the participants did not have as many chances to avoid the back facing virtual agents as they did the front facing virtual agents. Therefore, we will be unable to draw fair comparisons between the avoidance decisions of the front facing agent's compared to the back facing agents.

4.2.3.2 Head Mounted Display Bias

We expect that our lack of distortion correction for the head mounted display and the head tracking latency of up to 89.67ms will introduce some degree of bias into the study. The latency of our completely wireless head mounted display solution could be compared to commercial wired variants such as the HTC Vive or the Oculus Rift, which achieve reported latencies of approximately 20-30ms(depending on the application and software optimisation). It would not be unreasonable to suggest that there may be some qualitative difference in avoidance decision if the participant is extremely uncomfortable inside the virtual world. On a scale of 1 to 7, where 7 is no motion sickness or disorientation, the participants scored an average of 4.5/7. We feel that while not terrible, this score may be reason to suspect some additional bias in our results.

4.2.3.3 Combination of All Tests: Through or Around

Combining the decision data from each of the 4 tests; normal appearance + high density, normal appearance + low density, social-link appearance + high density and social-link appearance + low Density. We a found that 60.8% of participants went around the front facing virtual agent groups, while 39.2% of participants went through the front facing virtual agent groups. The t-Test reports that the participants decisions to go through or around the front facing virtual agent groups is not statistically significantly different; p=0.081(Figure 4-17).

t-Test: Two-Sample Assuming Unequal Variances		
	Around-Facing	*Through-Facing*
Mean	3.111111111	2
Variance	0.861111111	2.25
Observations	9	9
Hypothesized Me	0	
df	13	
t Stat	1.889822365	
P(T<=t) one-tail	0.040643077	
t Critical one-tail	1.770933396	
P(T<=t) two-tail	0.081286153	
t Critical two-tail	2.160368656	

Figure 4-17: T-Test going through or around front facing virtual agent groups.

56.25% of the participants navigated around the back facing virtual agent groups, whilst 43.75% navigated through the back facing virtual agents. The t-Test reports that the participants decisions to go through or around the back facing virtual agent groups is not statistically significantly different; p=0.63(Figure 4-18).

t-Test: Two-Sample Assuming Unequal Variances		
	Around-Back	*Through-Back*
Mean	1	0.777777778
Variance	1.25	0.694444444
Observations	9	9
Hypothesized Mean	0	
df	15	
t Stat	0.478091444	
P(T<=t) one-tail	0.31973905	
t Critical one-tail	1.753050356	
P(T<=t) two-tail	0.6394781	
t Critical two-tail	2.131449546	

Figure 4-18: T-Test going through or around back facing virtual agent groups.

4.2.3.4 High Density; Social and Normal Appearance: Around Front Facing

We a found that 60% of participants went around the front facing normal appearing virtual agent groups, while 40% of participants went around the front facing social-link appearing virtual agent groups. The t-Test reports that the participants decisions to go around the normal appearing virtual agent groups and social-link appearing virtual agent groups is not significantly different; p=0.39(Figure 4-19).

t-Test: Two-Sample Assuming Unequal Variances		
	(High)Around-Facing(Normal)	*(High)Around-Facing(Social)*
Mean	1	0.666666667
Variance	0	1.25
Observations	9	9
Hypothesized Mean Di	0	
df	8	
t Stat	0.894427191	
P(T<=t) one-tail	0.19860192	
t Critical one-tail	1.859548038	
P(T<=t) two-tail	0.397203841	
t Critical two-tail	2.306004135	

Figure 4-19: T-Test, going around: high density; normal appearance vs social-link appearance, for front facing virtual agent groups.

4.2.3.5 High Density; Social and Normal Appearance: Around Back Facing

We a found that 75% of participants went around the back facing normal appearing virtual agent groups, while 25% of participants went around the back facing social-link appearing virtual agent groups. The t-Test reports that the participants decisions to go around the normal appearing virtual agent groups and social-link appearing virtual agent groups is not significantly different; p=0.28(Figure 4-20).

t-Test: Two-Sample Assuming Unequal Variances		
	(High)Around-Back(Normal)	*(High)Around-Back(Social)*
Mean	0.333333333	0.111111111
Variance	0.25	0.111111111
Observations	9	9
Hypothesized Mean Di	0	
df	14	
t Stat	1.109400392	
P(T<=t) one-tail	0.142975502	
t Critical one-tail	1.761310136	
P(T<=t) two-tail	0.285951005	
t Critical two-tail	2.144786688	

Figure 4-20: T-Test, going around: high density; normal appearance vs social-link appearance, for back facing virtual agent groups.

4.2.3.6 High Density; Social and Normal Appearance: Through Front Facing

We a found that 50% of participants went through the front facing normal appearing virtual agent groups, while 50% of participants went through the front facing social-link appearing virtual agent groups. The t-Test reports that the participants decisions to go through the normal appearing virtual agent groups and social-link appearing virtual agent groups is not significantly different; p=1(Figure 4-21).

t-Test: Two-Sample Assuming Unequal Variances

	(High)Through-Facing(Normal)	(High)Through-Facing(Social)
Mean	0.444444444	0.444444444
Variance	0.527777778	1.027777778
Observations	9	9
Hypothesized Mean Difference	0	
df	15	
t Stat	0	
P(T<=t) one-tail	0.5	
t Critical one-tail	1.753050356	
P(T<=t) two-tail	1	
t Critical two-tail	2.131449546	

Figure 4-21: T-Test, going through: high density; normal appearance vs social-link appearance, for front facing virtual agent groups.

4.2.3.7 High Density; Social and Normal Appearance: Through Back Facing

We a found that 0% of participants went through the back facing normal appearing virtual agent groups, while 100% of participants went through the back facing social-link appearing virtual agent groups. The t-Test reports that the participants decisions to go through the normal appearing virtual agent groups and social-link appearing virtual agent groups is not significantly different; p=1(Figure 4-22).

t-Test: Two-Sample Assuming Unequal Variances

	(High)Through-Back(Normal)	(High)Through-Back(Social)
Mean	0	0.111111111
Variance	0	0.111111111
Observations	9	9
Hypothesized Mean Difference	0	
df	8	
t Stat	-1	
P(T<=t) one-tail	0.173296754	
t Critical one-tail	1.859548038	
P(T<=t) two-tail	0.346593507	
t Critical two-tail	2.306004135	

Figure 4-22: T-Test, going through: high density; normal appearance vs social-link appearance, for back facing virtual agent groups.

4.2.3.8 Low Density; Social and Normal Appearance: Around Front Facing

We a found that 15.3% of participants went around the front facing normal appearing virtual agent groups, while 84.6% of participants went around the front facing social-link appearing virtual agent groups. The t-Test reports that the participants decisions to go around the normal appearing virtual agent groups and social-link appearing virtual agent groups is significantly different; p=0.002(Figure 4-23).

t-Test: Two-Sample Assuming Unequal Variances		
	(Low)Around-Facing(Normal)	*(Low)Around-Facing(Social)*
Mean	0.222222222	1.222222222
Variance	0.194444444	0.444444444
Observations	9	9
Hypothesized Mean Difference	0	
df	14	
t Stat	-3.753259453	
P(T<=t) one-tail	0.001069777	
t Critical one-tail	1.761310136	
P(T<=t) two-tail	0.002139554	
t Critical two-tail	2.144786688	

Figure 4-23: T-Test, going around: low density; normal appearance vs social-link appearance, for front facing virtual agent groups.

4.2.3.9 Low Density; Social and Normal Appearance: Around Back Facing

We a found that 40% of participants went around the back facing normal appearing virtual agent groups, while 60% of participants went around the back facing social-link appearing virtual agent groups. The t-Test reports that the participants decisions to go around the normal appearing virtual agent groups and social-link appearing virtual agent groups is not significantly different; p=0.62(Figure 4-24).

t-Test: Two-Sample Assuming Unequal Variances		
	(Low)Around-Back(Normal)	*(Low)Around-Back(Social)*
Mean	0.222222222	0.333333333
Variance	0.194444444	0.25
Observations	9	9
Hypothesized Mean Difference	0	
df	16	
t Stat	-0.5	
P(T<=t) one-tail	0.311940778	
t Critical one-tail	1.745883676	
P(T<=t) two-tail	0.623881555	
t Critical two-tail	2.119905299	

Figure 4-24: T-Test, going around: low density; normal appearance vs social-link appearance, for back facing virtual agent groups.

4.2.3.10 Low Density; Social and Normal Appearance: Through Front Facing

We a found that 70% of participants went through the front facing normal appearing virtual agent groups, while 30% of participants went through the front facing social-link appearing virtual agent groups. The t-Test reports that the participants decisions to go through the normal appearing virtual agent groups and social-link appearing virtual agent groups is not significantly different; p=0.062(Figure 4-25).

t-Test: Two-Sample Assuming Unequal Variances		
	(Low)Through-Facing(Normal)	*(Low)Through-Facing(Social)*
Mean	0.777777778	0.333333333
Variance	0.194444444	0.25
Observations	9	9
Hypothesized Mean Difference	0	
df	16	
t Stat	2	
P(T<=t) one-tail	0.031385982	
t Critical one-tail	1.745883676	
P(T<=t) two-tail	0.062771964	
t Critical two-tail	2.119905299	

Figure 4-25: T-Test going through: low density; normal appearance vs social-link appearance for front facing virtual agent groups.

4.2.3.11 Low Density; Social and Normal Appearance: Through Back Facing

We a found that 50% of participants went through the back facing normal appearing virtual agent groups, while 50% of participants went through the back facing social-link appearing virtual agent groups. The t-Test reports that the participants decisions to go through the normal appearing virtual agent groups and social-link appearing virtual agent groups is not significantly different; p=1(Figure 4-26).

t-Test: Two-Sample Assuming Unequal Variances		
	(Low)Through-Back(Normal)	*(Low)Through-Back(Social)*
Mean	0.333333333	0.333333333
Variance	0.25	0.25
Observations	9	9
Hypothesized Mean Difference	0	
df	16	
t Stat	0	
P(T<=t) one-tail	0.5	
t Critical one-tail	1.745883676	
P(T<=t) two-tail	1	
t Critical two-tail	2.119905299	

Figure 4-26: T-Test going through: low density; normal appearance vs social-link appearance for back facing virtual agent groups.

4.2.3.12 Velocity of Participants

We performed the experiment expecting to observe the participants moving slower in the high density tests than the low density tests. However, this is not the case with an average velocity of 0.65m/s for the low density social-link appearance experiments and 0.67m/s for the high density social-link appearance experiments. The normal appearance experiments are similar with an average velocity of 0.61m/s for the low density and 0.63/s for the high density. The reason for the difference is possibly due to the high density tests not having enough virtual agents present. In addition, during the high density experiment the virtual agents formed 2 lanes; one moving towards the participant and the other moving in the same direction (Figure 4-27).The majority of the participants (90%) actually exhibited some degree of crowd following behaviour where they followed the virtual agent groups moving in the same direction they needed to go. The majority of the participants exhibiting following behaviour means that they did not have to spend velocity navigating around oncoming agents like they did in the low density experiment.

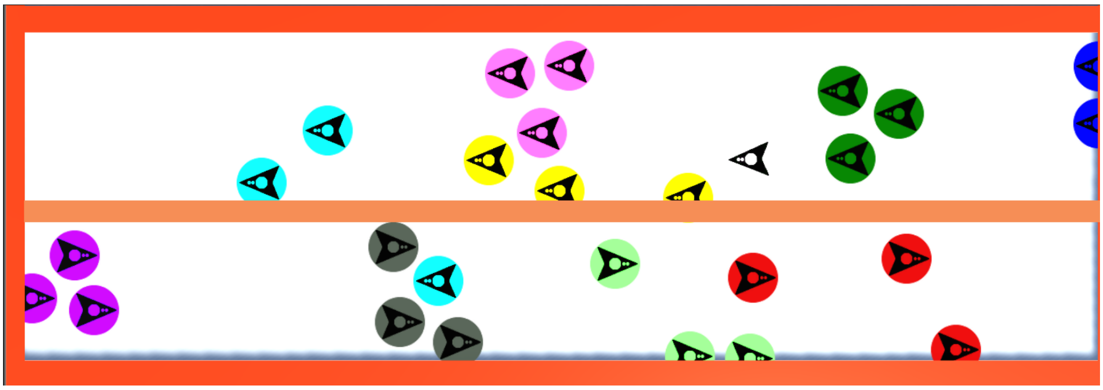

Figure 4-27: High density virtual agent lane formations and following behaviour.

5 Discussion and Comparison

As a result from conducting our virtual reality experiment in chapter 4.2 we have confirmed that our virtual reality framework is capable of observing qualitatively similar results to previous researchers. Bruneau observed his participants going around the front facing crowds with a social-link 54.4% of the time, he also found this to be statistically significant [12]. We also observed this behaviour in our low density experiment where 85% of our participants decided to go around the virtual agent groups with an easily visible social-link, our results were also statistically significant. We observed a similar correlation of less participants going through the front facing virtual agent groups with a social-link appearance. With only 30% of participants going through the front facing virtual agent groups with a social-link. Although, we found there to not be a statistical difference at the 95% confidence level (alpha=0.05). However, there is a statistical difference at the 93% confidence level (alpha=0.07).   We did not see this trend continue in the high density test or when we combined the low density test results with the high density test results. We expect this to be due to the majority of the participants in the high density tests not putting themselves in a position to need to be marked down as going around the oncoming front facing agents, as 90% of them conducted following behaviour of the virtual agents with the same direction of motion as them at one point or another during the virtual reality experiment (Figure 4-27). From these results we can conclude that during a low density environment people are able to make more navigation decisions than in a high density environment (where they often adopt following behaviour). While making more navigational decisions (low density) people are more likely to circumvent social-link appearing groups.

We did not see the same correlation of avoidance of back facing virtual people as we did with the front facing avoidance. This is most likely due to not having enough data, as discussed previously; the majority of the participants did not have as many chances to conduct avoidance around or through the back facing groups.

We observed a mean going around distance of 0.33m for the front facing agents and 0.35m for the back facing agents. Interestingly, this is confirming the modified personal space of virtual reality users observed in the literature [19], [26]. Real people observe a minimum distance between other real people of approximately 0.4m [28]. It should be noted that 70% of the participants reported “walking into” the virtual people during the interview after the experiment. However, the magnitude of the participants walking into the virtual people was actually just clipping them in most cases, only 30% of the participants actually fully walked through a virtual person. Only 13.3% of the 4 experiments conducted were affected by a participant completely walking into a virtual person. Therefore, we can conclude that the participants did have some degree of trouble controlling their virtual avatars around the virtual people. This might be explained by the distance compression effect introduced from viewing the world through a digital display.

We can confirm the digital compression effect from viewing the world through a digital display observed in the literature [15, 16, 17]. During the interview we asked the participants how long the virtual environment was. We received answers in the range of 5-14m, none of which is the actual distance of the length of the virtual environment which was 15m. The average of perceived virtual environment length was 9.7m. It should be noted that the distance compression effect could have been enhanced due to the lack of distortion correction on our stereoscopic camera.

During the experiment run’s we noticed that the participants where not moving 100% naturally. We can confirm previous research that reported virtual reality users moving with an increased gait instability [27].

Our Virtual reality framework was positively received with an enjoyment score of 5.6 out of 7(7 being very enjoyable).

6 Summary and Future Work

6.1 Summary

A completely wireless virtual reality framework that allows users to control virtual avatars by physically walking is becoming increasingly necessary as virtual reality technologies such as the Oculus Rift and HTC Vive are pushed into the mainstream market. Virtual reality is no longer an expensive tool only employed by the better funded researchers. To this end we proposed to create a novel virtual reality framework which lays the ground work for future researchers to utilize. The use of our virtual reality framework for research is validated through a virtual reality study which aims to help fill the knowledge gap of how individual pedestrians navigate through crowds.

In chapter 2 we focused on investigating the literature of using virtual reality systems for human behaviour research; exploring pedestrian group dynamics and the limitations of more conventional pedestrian data gathering methods.

In Chapter 3 we explored the implementation of our completely wireless virtual reality framework and the implementation of our virtual reality study investigating individual's avoidance groups. Our virtual reality framework consists of a Perception Neuron full body 18 Neuron inertial motion unit based motion capture kit, head mounted display in the form of a Homido with a Moto X 2nd Gen mobile device as the display; and a High end performance desktop computer. These components are all connected to each other wirelessly to allow completely un-restricted movements while immersed in the virtual environment. Our software framework includes the use of the A* PathFinding Project for Unity3D's RVO based Local Avoidance implementation for the controlling of our virtual agents. We developed a novel way to force the Local Avoidance agents into group formations based on the three group formations observed by Moussaid[7]. For the head tracking of the head mounted display we used the position and rotation values from the head mounted Neuron sensor from the Perception Neuron kit and applied that to our stereoscopic camera ripped from the Google Cardboard Unity3D integration package.

In Chapter 4 Phase 1 we explored the amount of drift that the Perception Neuron suit experienced with continuous use over a time period of 8 minutes. Due to inertial motion sensors susceptibility to drift over time it was imperative to know exactly how much the Perception Neuron suit drifts overtime when it is being used as the avatar controller for a 3D virtual reality simulation or game with a head mounted display. When designing the 3D environment we needed to take into account he drift that the suit creates to prevent the users from walking into real life walls or obstacles. Through our experimentation we developed two algorithms to determine the minimum amount of offset that the virtual world needed to be on both the X and Z axis.

In Chapter 4 Phase 2 we explored the use of our virtual reality framework to investigate how individual pedestrians navigate through virtual crowds. 10 participants volunteered for the experiment. We investigated the impact of realistic group formations based on Moussaids research [7]. We attempted to investigate the impact of both front and back facing agent groups as well as the impact of an easily visible social-link appearance on the participant's avoidance decisions.

In Chapter 5 we discussed the results from our virtual reality study investigating how individuals avoid groups. We discovered that our virtual reality framework was able to achieve qualitatively accurate results based on previous works in the area. Additionally, we found that we were able to further prove the distance compression effect, increased gait instability and modified personal space of people in virtual environments. Our Virtual reality framework was positively received with an enjoyment score of 5.6 out of 7(7 being very enjoyable).

6.2 Future work

The virtual reality framework developed in this thesis is currently the best way to obtain completely wireless-unrestricted virtual reality. However, it is true that the head mounted display in particular could be improved by using an Oculus rift or HTC Vive, but if money is an issue the Homido and smartphone combo offers a decent alternative. To this end future improvements of the framework would be the integration of either the Oculus Rift, HTC Vive or equivalent head mounted display.

As the technology in both the motion capture department and the head mounted display department mature using virtual reality for research purposes will become increasingly popular as we will begin to see some of the biases of virtual reality being reduced.

For the study of individual pedestrians navigating through groups we could further investigate the effects of the back facing virtual agents, as the data that we collected on this interaction was lacking. Additionally, Co-op virtual reality simulations could be employed where multiple individuals could navigate through a virtual crowd simultaneously- this would greatly reduce the amount of time needed to spend running experiments.

References

1. Olivier, A.-H., Bruneau, J., Cirio, G., & Pettré, J. (2014). A Virtual Reality Platform to Study Crowd Behaviors. Transportation Research Procedia, 2, 114–122. http://doi.org/10.1016/j.trpro.2014.09.015
2. Penny Marno(2002). Crowded - Macroscopic and Microscopic Models for pedestrian dynamics. https://www.reading.ac.uk/web/FILES/maths/NA_Report_4-02.pdf
3. Cheng, L., Yarlagadda, R., Fookes, C. B., & Yarlagadda, P. K. (2014). A review of pedestrian group dynamics and methodologies in modelling pedestrian group behaviours. World Journal of Mechanical Engineering, 1(1), 2–13. Retrieved from http://eprints.qut.edu.au/78716/
4. Johansson, A., Batty, M., Hayashi, K., Al Bar, O., Marcozzi, D., & Memish, Z. a. (2012). Crowd and environmental management during mass gatherings. The Lancet Infectious Diseases, 12(2), 150–156. http://doi.org/10.1016/S1473-3099(11)70287-0
5. Camillen, F., Caprì, S., Garofalo, C., Ignaccolo, M., Inturri, G., Pluchino, A., … Tudisco, S. (2009). Multi agent simulation of pedestrian behavior in closed spatial environments. In Science and Technology for Humanity (TIC-STH), 2009 IEEE Toronto International Conference (pp. 375–380). http://doi.org/10.1109/TIC-STH.2009.5444471
6. Pluchino, A., Garofalo, C., Inturri, G., Rapisarda, A., & Ignaccolo, M. (2014). Agent-based simulation of pedestrian behaviour in closed spaces: A museum case study. Jasss, 17, 1–14.
7. Moussaïd, M., Perozo, N., Garnier, S., Helbing, D., & Theraulaz, G. (2010). The walking behaviour of pedestrian social groups and its impact on crowd dynamics. PLoS ONE, 5(4), 1–7. http://doi.org/10.1371/journal.pone.0010047
8. Peters, C., & Ennis, C. (2009). Modeling groups of plausible virtual pedestrians. IEEE Computer Graphics and Applications, 29, 54–63. http://doi.org/10.1109/MCG.2009.69
9. Kretz, T., Grunebohm, A., Kaufman, M., Mazur, F., & Schreckenberg, M. (2006). Experimental study of pedestrian counterflow in a corridor. Journal of Statistical

Mechanics-Theory and Experiment, P10001. http://doi.org/10.1088/1742-5468/2006/10/P10001

10. Singh, H., Arter, R., Dodd, L., Langston, P., Lester, E., & Drury, J. (2009). Modelling subgroup behaviour in crowd dynamics DEM simulation. Applied Mathematical Modelling, 33(12), 4408–4423. http://doi.org/10.1016/j.apm.2009.03.020
11. Köster, G., Seitz, M., Treml, F., Hartmann, D., & Klein, W. (2011). On modelling the influence of group formations in a crowd. Contemporary Social Science, 6(3), 397–414. http://doi.org/10.1080/21582041.2011.619867
12. Bruneau, J., Olivier, A.-H., & Pettre, J. (2015). Going Through, Going Around: A Study on Individual Avoidance of Groups. IEEE Transactions on Visualization and Computer Graphics, 21(4), 520–528. http://doi.org/10.1109/TVCG.2015.2391862
13. Olivier, A.-H., Marin, A., Crétual, A., Berthoz, A., & Pettré, J. (2013). Collision avoidance between two walkers: role-dependent strategies. Gait & Posture, 38(4), 751–6. http://doi.org/10.1016/j.gaitpost.2013.03.017
14. Olivier, A. H., Marin, A., Crétual, A., & Pettré, J. (2012). Minimal predicted distance: A common metric for collision avoidance during pairwise interactions between walkers. Gait and Posture, 36(3), 399–404. http://doi.org/10.1016/j.gaitpost.2012.03.021
15. Loomis, J., & Knapp, J. (2003). Visual perception of egocentric distance in real and virtual environments. Virtual and Adaptive Environments, (11), 21–46. http://doi.org/10.1201/9781410608888
16. Renner, R. S., Velichkovsky, B. M., & Helmert, J. R. (2013). The perception of egocentric distances in virtual environments - A review. ACM Computing Surveys, 46(2), 1–40. http://doi.org/10.1145/2543581.2543590
17. Willemsen, P., Colton, M. B., Creem-Regehr, S. H., & Thompson, W. B. (2009). The effects of head-mounted display mechanical properties and field of view on distance judgments in virtual environments. ACM Transactions on Applied Perception, 6(2), 1–14. http://doi.org/10.1145/1498700.1498702
18. Banton, T., Stefanucci, J., Durgin, F., Fass, A., & Proffitt, D. (2005). The Perception of Walking Speed in a Virtual Environment. Presence, 14(4), 394–406. http://doi.org/10.1162/105474605774785262

19. Bailenson, J. N., Blascovich, J., Beall, A. C., & Loomis, J. M. (2003). Interpersonal Distance in Immersive Virtual Environments. Personality and Social Psychology Bulletin, 29(7), 819–833. http://doi.org/10.1177/0146167203253270
20. Helbing, D., & Molnár, P. (1995). Social force model for pedestrian dynamics. Physical Review E. http://doi.org/10.1103/PhysRevE.51.4282
21. Zheng, X., Zhong, T., & Liu, M. (2009). Modeling crowd evacuation of a building based on seven methodological approaches. Building and Environment, 44(3), 437–445. http://doi.org/10.1016/j.buildenv.2008.04.002
22. Karamouzas, I., & Overmars, M. (2012). Simulating and evaluating the local behavior of small pedestrian groups. IEEE Transactions on Visualization and Computer Graphics, 18(3), 394–406. http://doi.org/10.1109/TVCG.2011.133
23. Ismail, K., Sayed, T., & Saunier, N. (2010). Automated Collection of Pedestrian Data Using Computer Vision Techniques. Journal of the Transportation Research Board, (2198), 52–64. http://doi.org/10.3141/2198-07
24. Berg, J., Guy, S. J., Lin, M., & Manocha, D. (2011). Reciprocal n-Body Collision Avoidance. Springer Tracts in Advanced Robotics, 70, 3–19. http://doi.org/10.1007/978-3-642-19457-3_1
25. Fink, P.W., Foo, P.S., Warren, W.H., 2007. Obstacle avoidance during walking in real and virtual environments. ACM Trans. Appl. Percept. 4. Gerin-Lajoie, M., Richards, ´ C.L., Fung, J., McFadyen, B.J., 2008. Characteristics of personal space during obstacle circumvention in physical and virtual environments. Gait & Posture 27, 239 – 247.
26. Fink, P.W., Foo, P.S., Warren, W.H., 2007. Obstacle avoidance during walking in real and virtual environments. ACM Trans. Appl. Percept. 4. Gerin-Lajoie, M., Richards, ´ C.L., Fung, J., McFadyen, B.J., 2008. Characteristics of personal space during obstacle circumvention in physical and virtual environments. Gait & Posture 27, 239 – 247.
27. Hollman, J.H., Brey, R.H., Bang, T.J., Kaufman, K.R., 2007. Does walking in a virtual environment induce unstable gait?: An examination of vertical ground reaction forces. Gait & Posture 26, 289–294.
28. Rogers, J. A. (1972). Relationship between sociability and personal space preference at two different times of day. Perceptual and Motor Skills, 35, 519-526.

29. Woodman, O. J. (2007). An introduction to inertial navigation. University of Cambridge, Computer Laboratory, Tech. Rep. UCAMCL-TR-696, 14, 15.
30. McCarron, B. (2013). Low-Cost IMU Implementation via Sensor Fusion Algorithms in the Arduino Environment (Doctoral dissertation, California Polytechnic State University, San Luis Obispo).
31. T. Bawmann, "PERCEPTION NEURON UNITY HANDBOOK," Noitom, 18 9 2015. [Online]. Available: https://neuronmocap.com/sites/default/files/Perception%20Neuron%20Unity%20Handbook%200.2.4.pdf. [Accessed 26 5 2016]
32. Doc-Ok.org, "On the road for VR: Silicon Valley Virtual Reality Conference & Expo," Doc-Ok.org, 19 5 2015. [Online]. Available: http://doc-ok.org/?p=1239. [Accessed 26 05 2016].
33. MulticoreWare. (2016, unknown unknown). HEVC / H.265 Explained. Retrieved from http://x265.org/: http://x265.org/hevc-h265/
34. Granberg, A. (unknown, unknown unknown). astar/docs/local-avoidance.php. Retrieved from http://arongranberg.com/: http://arongranberg.com/astar/docs/local-avoidance.php
35. Van den Berg, J., Lin, M., & Manocha, D. (2008, May). Reciprocal velocity obstacles for real-time multi-agent navigation. In Robotics and Automation, 2008. ICRA 2008. IEEE International Conference on (pp. 1928-1935). IEEE.
36. Google. (2016, 05 18). Google Vr SDK for Unity. Retrieved from Developers.Google: https://developers.google.com/vr/unity/